Deep-Sea Research II 55 (2008) 1275–1290

Contents lists available at ScienceDirect

Deep-Sea Research II

journal homepage: www.elsevier.com/locate/dsr2

The transient oasis: Nutrient-phytoplankton dynamics and particle export in Hawaiian lee cyclones

Yoshimi M. Rii [a,*], Susan L. Brown [a], Francesco Nencioli [b], Victor Kuwahara [b], Tommy Dickey [b], David M. Karl [a], Robert R. Bidigare [c]

[a] Department of Oceanography, School of Ocean and Earth Science and Technology, University of Hawai'i, Honolulu, HI 96822, USA
[b] Ocean Physics Laboratory, University of California Santa Barbara, Santa Barbara, CA 93117, USA
[c] Hawai'i Institute of Marine Biology, Kaneohe, HI 96744, USA

ARTICLE INFO

Article history:
Accepted 25 January 2008
Available online 15 May 2008

Keywords:
Mesoscale eddies
Phytoplankton
Macronutrients
Photosynthetic pigments
Particle export
North Pacific Ocean

ABSTRACT

Macronutrients, photosynthetic pigments, and particle export were assessed in two eddies during the E-Flux I and III cruises to investigate linkages between biogeochemical properties and export flux in Hawaiian lee cyclonic eddies. Cyclone *Noah* (E-Flux I), speculated to be in the 'decay' stage, exhibited modest increases in macronutrients and photosynthetic pigments at the eddy center compared to ambient waters. Cyclone *Opal* (E-Flux III) also exhibited modest increases in macronutrient concentrations, but a 2-fold enhancement in total chlorophyll *a* (TChl *a*) concentration within the eddy center. As indicated by fucoxanthin concentrations, the phytoplankton community in the deep chlorophyll maximum (DCM) of *Opal* was comprised mainly of diatoms. During an 8-day time series in the center of *Opal*, TChl *a* concentration and fucoxanthin in the DCM decreased by ~50%, which was potentially triggered by silicic acid limitation. Despite the presence of a substantial diatom bloom, *Opal* did not deliver the expected export of particulate carbon and nitrogen, but rather a large biogenic silica export (~4-fold increase relative to export in surrounding waters). Results suggest that controls on the life cycle of a Hawaiian lee cyclone are likely a combination of physical (eddy dynamics), chemical (nutrient limitation), and biological (growth and grazing imbalance) processes. Comparisons between *Noah* and *Opal* and previously studied cyclones in the region point to a relationship between the spin-up duration of a cyclone and the resulting biological response. Nonetheless, Hawaiian lee cyclones, which strongly influence the biogeochemistry of areas 100's of km in scale in the subtropical North Pacific Ocean, still remain an enigma.

1. Introduction

Phytoplankton community structure in the Subtropical North Pacific Ocean (SNPO) is primarily influenced by the lack of inorganic macronutrient availability (nitrogen, N; phosphorus, P; and silicon, Si) in the upper euphotic zone. Minute organisms with high surface area-to-volume ratios, such as photosynthetic bacteria (i.e. *Prochlorococcus* spp.) and picophytoplankton (0.2–2 μm), are efficient at nutrient uptake and light harvesting and comprise the 'climax community' in the SNPO (Clements, 1916; Campbell and Vaulot, 1993; Anderson et al., 1996; Karl et al., 2001a). In a two-layer distribution typical of the SNPO, cyanobacteria (i.e. *Synechococcus* and *Prochlorococcus* spp.) dominate the mixed layer (~⩽50 m) and *Prochlorococcus* spp. and photosynthetic pico- and nanoeukaryotes (i.e. prymnesiophytes and pelagophytes) comprise the deep chlorophyll maximum (DCM, ~90–110 m) (Bidigare et al., 1990, 2008; Ondrusek et al., 1991; Letelier et al., 1993).

A standing stock of smaller phytoplankton suggest minimal particulate organic matter flux in the SNPO, since large eukaryotic phytoplankton are often reported to have a critical role in export production (Eppley, 1969; Goldman, 1993; Legendre and Le Fevre, 1995). Additionally, since organic matter production is controlled by the nutrient available in the lowest concentration relative to the needs of phytoplankton growth (Law of the Minimum, Justus von Liebig), lack of organic matter export in the SNPO has been attributed to N or P deficiencies in the euphotic zone (Karl et al., 2001a, b; Karl, 2002) and/or high rates of respiration (Laws et al., 2000). The input of fixed N into the nutrient-limited surface waters of the SNPO via the processes of nitrogen fixation and nitrification plays an important role in the N:P stoichiometry of available nutrient pools in the system. Due to varying supply rates, the SNPO community is reported to alternate between states of N and P limitation via El Niño-Southern Oscillation

* Corresponding author. Tel.: +1 808 956 7632; fax: +1 808 956 5308.
E-mail address: shimi@hawaii.edu (Y.M. Rii).

0967-0645/$ - see front matter © 2008 Elsevier Ltd. All rights reserved.
doi:10.1016/j.dsr2.2008.01.013

(ENSO) forcing (Karl et al., 2001b; Karl, 2002). Thus, the provenance of nutrient supply in the SNPO has significant implications for productivity, subsequent nutrient limitation, and particulate matter export.

In this region where regenerated production is the status quo, aperiodic displacements of isopycnal surfaces by Rossby waves and mesoscale eddies have been reported to drive an influx of "new" nutrients into the euphotic zone, generating significant variability in plankton biomass and processes in the surface ocean (Eppley and Peterson, 1979; Falkowski et al., 1991; McGillicuddy and Robinson, 1997; McNeil et al., 1999; Cipollini et al., 2001; Seki et al., 2001; Siegel, 2001; Uz et al., 2001; Bidigare et al., 2003; Vaillancourt et al., 2003; Sakamoto et al., 2004). First baroclinic mode, cold-core, cyclonic eddies are ephemeral yet frequent occurrences during persistent trade wind conditions in the lee of the 'Alenuihaha Channel between the islands of Maui and Hawai'i (Patzert, 1969; Bienfang et al., 1990; Lumpkin, 1998; Dickey et al., 2008). Intensified northeasterly trade winds and island topography contribute to the formation of these cyclonic eddies to the north of the channel (Lumpkin, 1998; Chavanne et al., 2002; Calil et al., 2008; Dickey et al., 2008). The upward displacement of isopycnal surfaces elicits an ecosystem response by (1) relocating seed populations of nutrient-replete, light-limited phytoplankton to areas of higher light intensity and/or, (2) increasing the supply of growth-limiting nutrients to the well-lit zone for light-replete, nutrient-limited phytoplankton. Increased rates of biological processes such as nutrient uptake and carbon fixation often induce substantial phytoplankton blooms in which larger photosynthetic eukaryotes dominate. Therefore, eddies have been hypothesized to enhance rates of carbon export by means of altered food web dynamics namely increased macrozooplankton grazing and subsequent fast-sinking fecal pellets (Falkowski et al., 1991; Goldman, 1993; Legendre and Le Fevre, 1995; Seki et al., 2001; Bidigare et al., 2003).

Variations in eddy dynamics have been attributed to different developmental stages and varying time scales in physical, biological, and biogeochemical responses (Sweeney et al., 2003; Flierl and McGillicuddy, 2002). Sweeney et al. (2003) suggested that the life cycle of a cyclonic eddy is divided into three stages: 'intensification,' 'mature,' and 'decay.' Nutrient injection into the euphotic zone stimulates a biological response during 'intensification,' after which a cyclone reaches its 'mature' stage as it attains its maximum tangential velocity, production rate, and highest biomass. After some time, the induced biological response is expected to generate increased export. As wind speed diminishes or the eddy migrates from the area of strongest winds in the 'Alenuihaha Channel, a 'mature' cyclone subsides into the 'decay' stage as the doming of the isopycnals relaxes and tangential velocity decreases. At this time, the eddy undergoes a significant physical and biological transformation towards ambient conditions, leaving behind a high export signal as the remains of an eddy-induced bloom (Patzert, 1969; Sweeney et al., 2003).

For an eddy-pumping mechanism to contribute significantly to export production in the SNPO, a means to restore isopycnal nutrient concentrations on relatively short time-scales must exist (Garçon et al., 2001; Lewis, 2002; Sakamoto et al., 2004). Essentially, the 'pumping' of water from below would only occur once, and nutrients should reach the euphotic zone only as the eddy forms, not as it matures or propagates. Thus, if nutrients on a deeper isopycnal surface are depleted, the biological response of the next eddy would be minimized as less nutrients are injected into the euphotic zone. Therefore, the effectiveness of the eddy mechanism depends on the relative time and vertical length scales of nutrient regeneration and the time period of eddy recurrence in the same general location (Garçon et al., 2001; Lewis, 2002). To date, only a handful of studies have focused on the influence of cyclonic eddies on carbon export (Honjo et al., 1999; Bidigare et al., 2003; Sweeney et al., 2003). The impetus for the E-Flux project was the sizeable potential for cyclonic eddies to increase the transfer of organic carbon to the mesopelagic zone in the oligotrophic North Pacific Ocean. The present study assessed the spatial and temporal variability in macronutrient and phytoplankton distributions and subsequent influences on particulate matter export within Hawaiian lee cyclones. Age-specific variability was examined with respect to the conceptual model described by Sweeney et al. (2003). Ecological predictions of their model were tested using three biological parameters: dissolved macronutrients, phytoplankton community composition, and particulate matter export.

2. Methods

2.1. Eddy tracking

The seasonal intensification of trade winds through the 'Alenuihaha Channel make the lee of Hawai'i an ideal natural laboratory for studying cyclonic eddies. Cyclone *Noah* was studied during E-Flux I (4–22 November 2004) aboard the University of Hawai'i's R/V *Ka'imikai-O-Kanaloa*; Cyclone *Opal* was surveyed during E-Flux III (10–28 March 2005) aboard Oregon State University's R/V *Wecoma*. Three main methods were used to determine the locations and track the eddies during ship-based observations. As our first method, satellite-derived measurements of sea-surface temperature (SST) obtained from Geostationary Operational Environmental Satellites (GOES) radiance sensors (via the EddyWatch section of the NOAA CoastWatch Program, http://oceanwatch.pifsc.noaa.gov/) and NASA's Moderate Resolution Imaging Spectroradiometer (MODIS) were sent electronically to the research vessels and used to determine initial sampling locations. These SST measurements also aided in the placement of drifters in proximal centers as well as in tracking the movements of the eddies during our observations. Secondly, surface currents measured with a 153-kHz RDI acoustic Doppler current profiler (ADCP) were tracked to monitor the locations and to determine the spatial dimensions of the eddies. Thirdly, two drifters were deployed: a surface drifter (OPL drifter) with a 1.5-m cylindrical foam core and a 1-m cross-shaped drogue, which tracked the fluid motion of the eddies and was able to obtain a near real-time, Lagrangian time series of temperature measurements from surface to 150 m at 10-m intervals; and a METOCEAN bio-optical surface drifter that acquired temporal measurements of drifter positions, barometric pressure, air temperature, SST, and fluorescence. A drifting sediment trap array (Section 2.2.2) also proved to be useful as an ad hoc Lagrangian drifter for tracking general patterns of eddy motion. More details on eddy tracking during specific cruises are described in Dickey et al. (2008).

2.2. Sample collection

2.2.1. "Star" transects and process stations

A "star" sampling strategy allowed three-dimensional spatial characterization of eddy variability. This also provided a four-dimensional (x, y, z, t) data set for investigating linkages between nutrient inputs, biological response, and the downward flux of particulate carbon. At least two replicate stations were sampled in the centers of Cyclones *Noah* and *Opal* and at control (OUT) stations, which were far-field locations unaffected by eddy dynamics. Hydrographic data (temperature, salinity, pressure, density, fluorescence, and oxygen) and *in situ* water samples were acquired from a SeaBird SBE 9/11+ CTD system plus

rosette sampler. Photosynthetically available radiation (PAR) (μmol photons m^{-2} s^{-1}) was measured with an attached sensor and the bottom of the euphotic zone was calculated as the depth at which irradiance measurements collected during daylight hours was 1% of the surface light level (LL). Coefficients were derived by correlating daytime 1% LL depths to mean total chlorophyll *a* (TChl *a*) concentrations between the surface and 1% LL depths, and the relationship was used to determine 1% LL depths for casts collected at night (Morel, 1988). Details concerning sampling strategies and physical and bio-optical measurements for E-Flux I are given in Dickey et al. (2008) and Kuwahara et al. (2008) and for E-Flux III in Dickey et al. (2008) and Nencioli et al. (2008).

For both eddies, a single "star" was sampled which consisted of multiple transects across the eddy with stations ~18 km apart. In *Noah*, samples for macronutrients and photosynthetic pigments were taken at depth intervals from 0 to 500 m during Transect 3 ('money run,' casts 27–34, 36, 37), with the 'center' of the eddy between casts 31 and 32 according to ADCP current velocities and density profiles (Fig. 1A) (Kuwahara et al., 2008). Samples in *Opal* were taken at depth intervals from 0 to 350 m during Transect 3 ('money run,' casts 13–18, 19A, 22–25) with cast 19A being the 'center' of the eddy (Fig. 1B) (Nencioli et al., 2008).

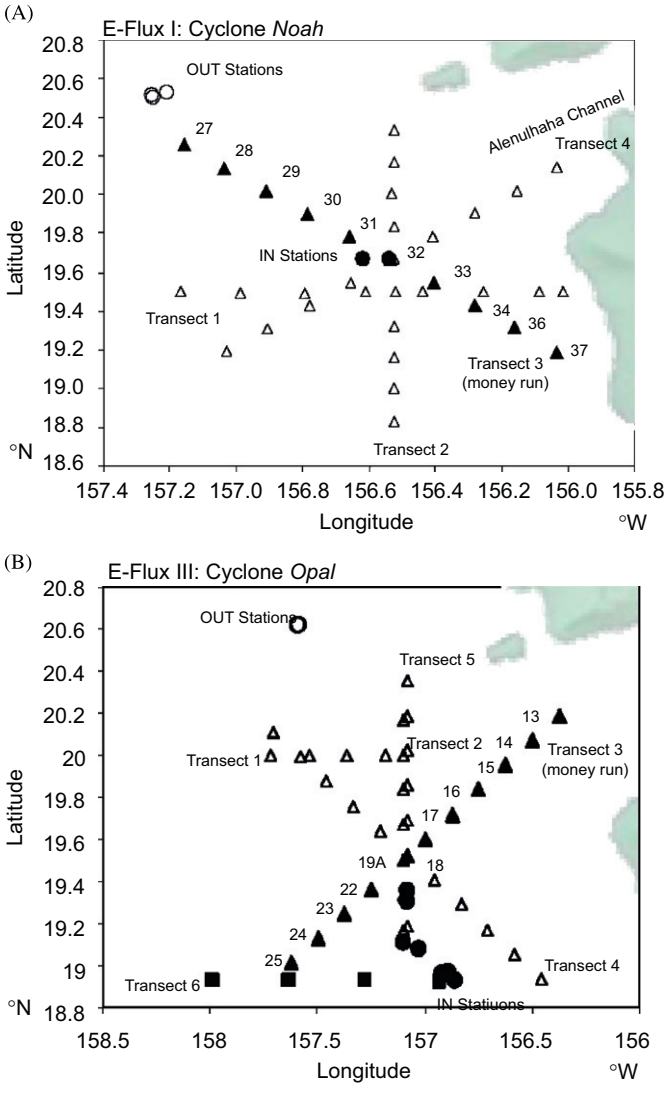

Fig. 1. "Star" sampling scheme (triangles) and process stations (circles) for E-flux I (A) and III (B). Closed triangles indicate Transect 3 on which all biogeochemical samples were taken. IN (closed circles) and OUT (open circles) process stations and Transect 6 (closed squares) are denoted.

Process stations in *Noah* were sampled for macronutrients (0–1000 m; IN = 2, OUT = 2) and photosynthetic pigments (0–150 m; IN = 2, OUT = 3). Process stations (IN = 7, OUT = 3) in the center of *Opal* were sampled daily (16–22 March) for pigments and six of these stations (17–22 March) were sampled for macronutrients. Size-fractionated pigment samples for both *Noah* (IN = 3, OUT = 3) and *Opal* (IN = 3, OUT = 2) were taken at the ~11% (base of mixed layer) and ~43% (in mixed-layer) light levels. Size-fractionated pigment samples were also collected from the DCM along Transect 6 of *Opal* (casts 97, 99, 101, 103) extending from the center of the eddy (cast 97) towards the edge (~100 km). A single depth profile to 1000 m was sampled for suspended biogenic silica both inside and outside of *Opal*.

Water samples for macronutrient concentrations were collected in acid-washed 125-mL HDPE bottles, immediately frozen (−20 °C), and stored upright until analysis. Photosynthetic pigment samples were collected into brown, narrow-mouthed 2-L HDPE bottles, immediately vacuum-filtered onto 25-mm GF/F filters for total pigment biomass or polycarbonate filters (0.2, 2, and 18 μm) for size-fractionated biomass, and stored in liquid nitrogen until analysis. Water for suspended biogenic silica analysis was collected in clear, narrow-mouthed 2-L HDPE bottles, immediately vacuum-filtered onto 25-mm 0.8-μm polycarbonate filters, and kept at −20 °C until analysis.

2.2.2. Sediment trap array

A particle interceptor sediment trap array, or PITs, was suspended at 150 m for a minimum of 3 days in and out of each eddy. The array consisted of 12 cylindrical polycarbonate collector tubes with a 0.0039 m^2 mouth opening fitted with baffles of 25-mm diameter cells (Knauer et al., 1979; Karl et al., 1996). Tubes were affixed to a PVC cross frame attached to a 12-mm POLYPRO line.

Collector tubes were filled with high-density seawater brine solution to prevent loss of preservative during deployment and loss of sample during recovery. The brine solution was a mixture of 1% formalin and 2.5 kg NaCl dissolved in 50 L of filtered surface seawater. Upon recovery of the array, tubes containing the collected particulate matter were pre-filtered through a 335-μm Nitex mesh to remove accidental zooplankton swimmers. Overlying seawater from each tube was removed with a pipette and the brine solution alone was filtered for specific analyses.

2.3. Sample analysis

2.3.1. Inorganic macronutrients

Samples for nitrate+nitrite (N+N), phosphate, and silicic acid were sent to Oregon State University and were analyzed using a continuous segmented flow system consisting of components of both a Technicon Autoanalyzer II™ and an Alpkem RFA 300™ (Gordon et al., 1994). Analysis for N+N used the basic method of Armstrong et al. (1967) with modifications to improve the precision and ease of operation. The phosphate method was a modification of the molybdenum blue procedure of Bernhardt and Wilhelms (1967). Silicic acid was measured using the method of Armstrong et al. (1967) as adapted by Atlas et al. (1971). The precision of analyses was a function of the concentration range of each macronutrient: N+N = 0.132 μM/mV, phosphate = 0.132 μM/mV, and silicic acid = 0.482 μM/mV. Detection limits for these specific sample runs were as follows: nitrate = 0.14 μM, nitrite = 0.02 μM, phosphate = 0.0075 μM, and silicic acid = 0.35 μM (J. Jennings, pers. comm.).

2.3.2. Pigments

Chlorophyll and carotenoid pigments were analyzed at the University of Hawai'i on a Varian 9012 HPLC system using methods described in Bidigare et al. (2005). Filters were extracted in 3 mL of HPLC-grade acetone in culture tubes along with 50 μL of an internal standard (canthaxanthin) at 4 °C for 24 h. Photosynthetic pigments were separated on a reverse-phase Waters Spherisorb® 5-μm ODS-2 ($4.6 \times 250\,mm^2$) C_{18} column with a corresponding guard cartridge ($7.5 \times 4.6\,mm^2$) and a Timberline column heater (26 °C) (Wright et al., 1991; Bidigare et al., 2005). Separated pigments were detected and the data were transferred to the attached computer system using SpectraSYSTEM Thermo Separation Products UV2000 (dual wavelength UV/VIS) and FL2000 (fluorescence) detectors. Pigment identifications were based on absorbance spectra, co-chromatography with standards, and relative retention time. Peak identity was determined by comparing retention times with a chlorophyll *a* standard and representative culture extracts. Spectra-Physics WOW® software was used to conservatively calculate peak area (Mantoura and Llewellyn, 1983; Wright et al., 1991; Bidigare and Trees, 2000). A dichromatic equation was used to resolve mixtures of monovinyl and divinyl chlorophyll *a* spectrally (Bidigare and Trees, 2000). Abbreviations for diagnostic photosynthetic pigments separated in this study are provided in Table 1.

2.3.3. Suspended biogenic silica

Suspended biogenic silica (BSi) was analyzed at the University of Hawai'i according to methods specified in Paasche (1980) and Brzezinski and Nelson (1995). Samples were digested in 0.2 N NaOH solution and developed using a time-sensitive dilution technique with ammonium molybdate and a reducing agent. The percent transmittance of the developed sample was read on a spectrophotometer at 810 nm and compared against a standard curve made with a 2.5-mM silicate stock solution (Na_2SiF_6).

Table 1
Abbreviations and taxonomic affinities of photosynthetic pigments separated in this study using HPLC

Pigment name	Abbreviation	Primary pigment in
Total chlorophyll *a*[a]	TChl *a*	All phytoplankton
Monovinyl chlorophyll *a*	MVChl *a*	All phytoplankton (except *Prochlorococcus* spp.)
Divinyl chlorophyll *a*	DVChl *a*	*Prochlorococcus* spp.
Monovinyl chlorophyllide *a*	MVChld *a*	Senescent diatoms
Monovinyl plus divinyl chlorophyll *b*	TChl *b*	*Prochlorococcus* spp.
Chlorophyll *c*-like pigments	TChl *c*	Chromophytes
19′-Butanoyloxyfucoxanthin	But-fuco	Pelagophytes
19′-Hexanoyloxyfucoxanthin	Hex-fuco	Prymnesiophytes
Fucoxanthin	Fuco	Diatoms
Peridinin	Per	Dinoflagellates
Prasinoxanthin	Pras	Prasinophytes
Violaxanthin	Viola	Chrysophytes
Diadinoxanthin	DDX	Chromophytes
Alloxanthin	Allox	Cryptophytes
Diatoxanthin	DTX	Minor pigment in chromophytes
Zeaxanthin	Zeax	Cyanobacteria
β,ε-Carotene	α-Car	*Prochlorococcus* spp., cryptophytes
β,β-Carotene	β-Car	All phytoplankton groups (except *Prochlorococcus* spp.)

Chromophytes are defined as those microalgae that possess the accessory pigment chlorophyll *c*.
Pigment descriptions from Jeffrey and Vesk (1997).
[a] TChl *a* = MVChl *a*+DVChl *a*+MVChld *a*.

2.3.4. Particulate export

Sediment trap tubes were analyzed for particulate carbon, nitrogen, phosphorus and silica, photosynthetic pigments, and microscopy. Six filters (three samples, three blanks) of particulate carbon and nitrogen collected per trap deployment were stored in a shipboard freezer (−20 °C) and analyzed on a Carlo Erba Elemental Analyzer (model NC2500) interfaced with a Finnigan DeltaS ion ratio-monitoring mass spectrometer (Sharp, 1974). Filters for particulate phosphorus were analyzed following the methods of Strickland and Parsons (1972). Filters for photosynthetic pigments of exported material were analyzed using methods described above. During pigment extraction, grinding of the filters was necessary to suspend all sediment and organic material from the filters. Filters for particulate biogenic silica were analyzed as follows using the methods of DeMaster (1981). Time course subsamples were measured colorimetrically to distinguish lithogenic silica from biogenic silica, which dissolves more readily than compounds of mineral origin according to the method described by DeMaster (1981). In addition, trap material was examined by epifluorescence microscopy as described by Scharek et al. (1999b) and Brown et al. (2003).

3. Results

3.1. Cyclone Noah

Cyclone *Noah* first appeared in GOES and MODIS SST imagery between 13 and 21 August 2004, downwind of the 'Alenuihaha Channel. *Noah* intensified and moved southeast into the lee of Hawai'i over the next 2 months. The E-Flux group encountered *Noah* (5–17 November 2004) within ~3 months of its appearance, and GOES SST imagery showed that its surface expression was elliptical in shape, possibly indicative of relaxation and decay (Kuwahara et al., 2008). During the 3 weeks of observations, *Noah* remained in the same approximate location (~20.1°N, 156.4°W). *Noah* disappeared from GOES imagery on ~21 December 2004, ~4 months after it first appeared. Given that only eddies with surface expressions can be detected via satellite and that subsurface features are often masked by near surface effects (i.e. diurnal heating and cooling, etc.), *Noah* (and presumably other eddies) likely spun up prior to satellite detection; thus all eddy ages should be viewed as approximate (for more details concerning satellite observations, see Dickey et al., 2008).

Physically, *Noah* appeared to be a fully developed cyclonic eddy (Kuwahara et al., 2008). *Noah* had a physical core with maximum tangential velocities (at 40 m depth) up to $80\,cm\,s^{-1}$ at 20–40 km from the center and a shallow (~200 m), semi-elliptical shape, which measured ~144 km in the major axis (in the northwest to southeast direction) and ~90 km in the minor axis. Angular velocity varied with distance from the center, indicating that solid body rotation did not occur beyond ~10 km from the estimated geometric center (Kuwahara et al., 2008). Though semi-elliptical in the upper 100 m, the layer below (100–140 m) was observed to be more circular and symmetric, suggesting that the upper layers were beginning to decay while the bottom layer remained as a cohesive body. More detail regarding *Noah*'s ellipticity and shape is discussed in Kuwahara et al. (2008). The isopycnal density surface of $\sigma{-}t_{24.0}$ ($\sigma_t = 24.0\,kg\,m^{-3}$) was displaced from 132 ± 8 m ($n = 7$) in ambient waters upwards to 83 ± 8 m ($n = 7$) at the eddy center. The depth of the euphotic zone, defined as the depth of 1% surface illumination, was 105 ± 2 m ($n = 9$) at the center of *Noah* relative to 111 ± 3 m ($n = 9$) in surrounding waters.

3.1.1. Macronutrient distributions

Dissolved inorganic macronutrient concentrations increased slightly within the eddy center in the upper 150 m compared to

surrounding waters (Fig. 2, Table 2). Contour plots of N+N, phosphate, and silicic acid followed the doming of isopycnal surfaces. N+N concentrations were just above the limit of detection at ~100 m in the center of *Noah* compared to ~120 m in surrounding waters, and were negligible in the upper water column above the $\sigma{-}t_{24.0}$ isopycnal surface (~85 m in the center). In the center of the eddy, N+N and phosphate concentrations were enhanced slightly in the euphotic zone (as indicated by the yellow line on the contour plots) and silicic acid concentrations were close to the limit of detection in the upper 50 m (Fig. 2).

Macronutrients were first integrated over 0–150 m both in and out of the eddy in order to compare the standing stock of nutrients in a given geometric mass of water. These values revealed 3.3-, 1.6-, and 1.3-fold increases for N+N, phosphate, and silicic acid concentrations, respectively, in *Noah* compared to surrounding waters (Table 2). Macronutrients were also integrated over the calculated depths of the euphotic zones in (0–110 m) and out (0–115 m) of *Noah* to assess nutrient availability and utilization by phytoplankton. Increases in these integrated values (3.7-, 1.4-, and 1.2-fold, Table 2) were similar to increases in values integrated over 0–150 m.

3.1.2. *Photosynthetic pigment biomarkers*

Water-column profiles of TChl *a* in and out of *Noah* did not show significant differences except for a slight upward displacement of the DCM by ~20 m (Fig. 3A). Contour plots of chlorophyll and carotenoid pigment biomarkers depict a similar upward displacement of the DCM, shadowing the doming of the isopycnal surfaces and remaining at the base of the euphotic zone

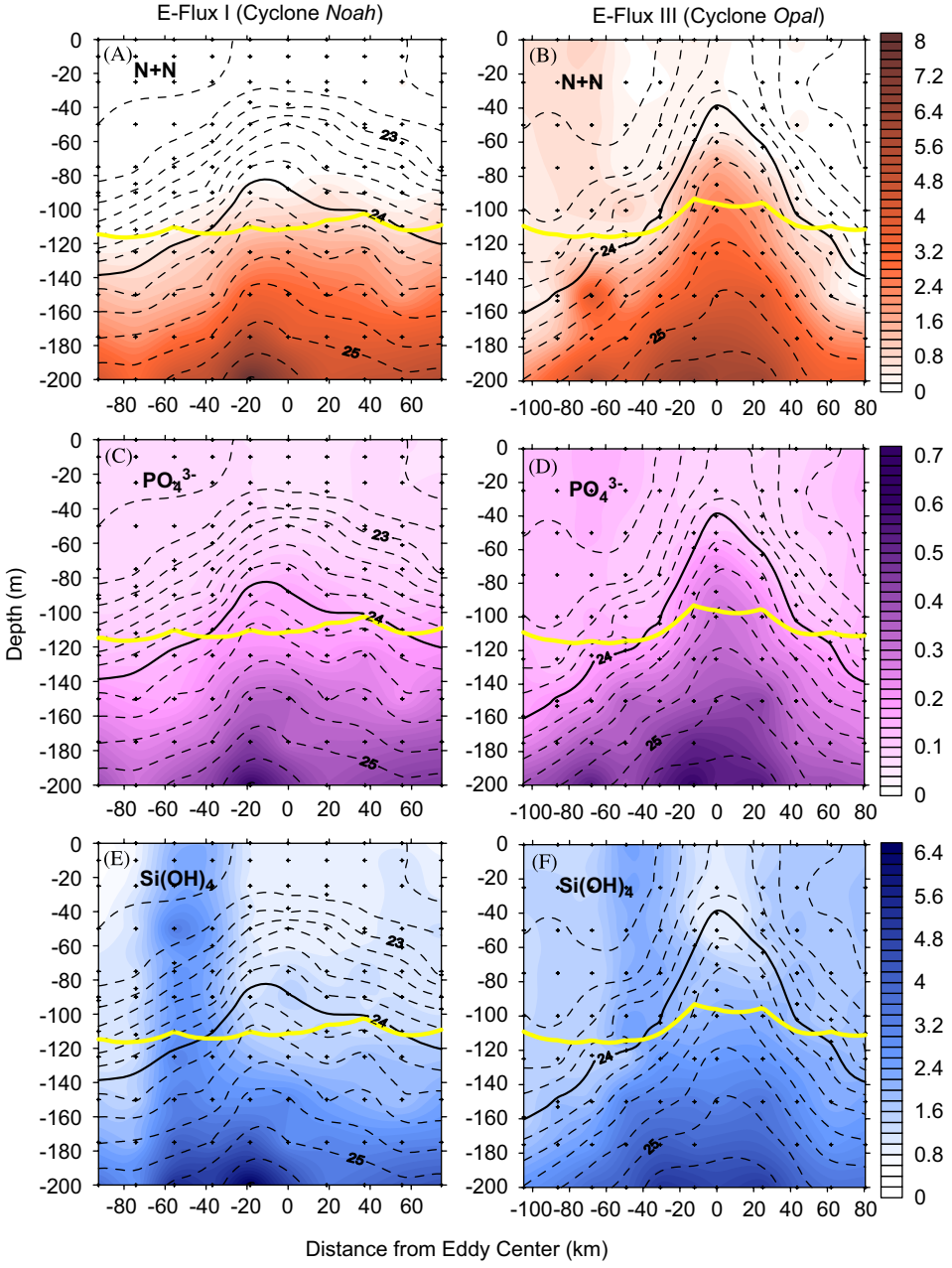

Fig. 2. Depth contours of N+N (μM, panels A, B), phosphate (PO_4^{3-}, μM, panels C, D), and silicic acid ($Si(OH)_4$, μM, panels E, F) in Cyclones *Noah* and *Opal* from Transect 3. Contours of isopycnal surfaces (σ–*t*, dotted lines), crosses indicating sampling depths, and a yellow line representing the depths of the euphotic zone (1% surface LL) are overlaid on each figure.

Table 2
Depth-integrated inorganic macronutrients during E-Flux I (Cyclone *Noah*) and E-Flux III (Cyclone *Opal*)

Parameter	E-Flux I			E-Flux III		
	Cyclone *Noah*			Cyclone *Opal*		
	IN ($n = 2$)	OUT ($n = 2$)	IN/OUT	IN ($n = 6$)	OUT ($n = 3$)	IN/OUT
0–150 m depth-integrated						
Nitrate+nitrite (mmol N m^{-2})	136 (18)	41.7 (3.9)	3.3	225 (18)	55.5 (1.4)	4.1
Phosphate (mmol P m^{-2})	26.5 (1.8)	16.5 (2.3)	1.6	32.0 (2.9)	17.3 (3.2)	1.8
Silicic acid (mmol Si m^{-2})	201 (25)	152 (29)	1.3	279 (55)	248 (44)	1.1
Euphotic zone depth-integrated (m)	0–110	0–115		0–100	0–115	
Nitrate+nitrite (mmol N m^{-2})	45.5 (4.8)	12.4 (5.8)	3.7	71.6 (13)	26.5 (0.8)	2.7
Phosphate (mmol P m^{-2})	15.6 (0.1)	10.8 (1.6)	1.4	14.5 (1.6)	10.7 (1.8)	1.4
Silicic acid (mmol Si m^{-2})	129 (9.7)	107 (22)	1.2	158 (25)	180 (25)	0.9

n Indicates the number of samples averaged and the values in columns indicate mean (range) for Cyclone *Noah* and mean (±s.d.) for Cyclone *Opal*. Mean values from E-Flux I: IN = IN Sta. 1–2, OUT = OUT Sta. 1–2; from E-Flux III: IN = IN Sta. 2–7, OUT = OUT Sta. 1–3. Euphotic zone depths were calculated as the depth of 1% LL.

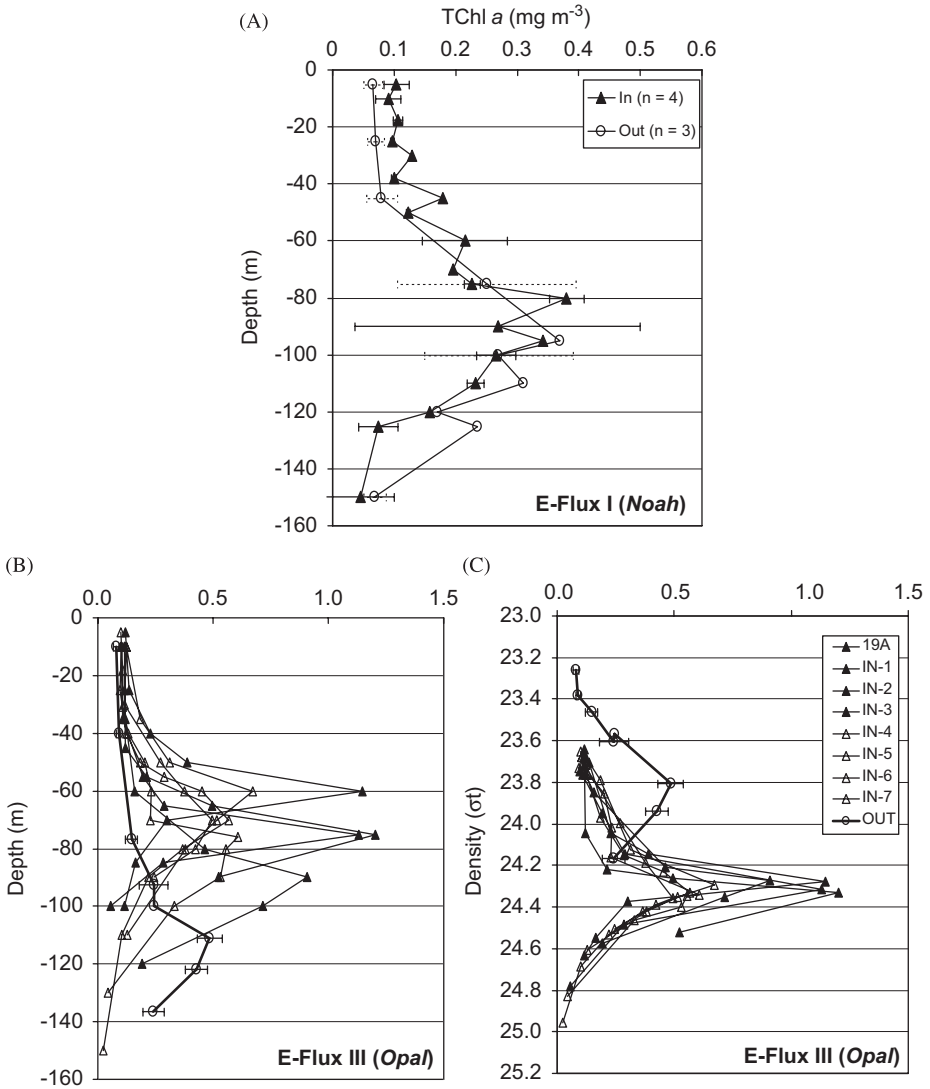

Fig. 3. Water-column profiles of TChl *a* concentration during E-Flux I (A) and III (B, C). Panel A: IN Sta. (dark triangles) are mean values (error bars = ±s.d.) of IN Sta. 1 and 2 and casts 31 and 32 from Transect 3. OUT Sta. (open circles) are mean values (error bars = ±s.d.) of OUT Sta. 1–3. Panels B (independent parameter is depth) and C (independent parameter is density) show the center station from Transect 3 (cast 19A) and IN Sta. 1–3 (dark triangles), IN Sta. 4–7 (open triangles), and mean values (error bars = ±s.d.) of OUT Sta. 1–3 (open circles).

(Figs. 4 and 5). Chlorophyll pigments TChl *a*, MVChl *a*, and DVChl *a* (biomarker for *Prochlorococcus* spp.) were not markedly enhanced in the center of the eddy relative to ambient waters (Fig. 4). Hex-fuco and But-fuco, carotenoid biomarkers for prymnesiophytes and pelagophytes, respectively, increased slightly at the periphery of the center of the eddy (Fig. 5(A), (C)). Cyanobacterial pigment Zeax (biomarker for *Synechococcus* and *Prochlorococcus* spp.) was concentrated in the mixed layer above the $\sigma-t_{24.0}$ isopycnal surface and remained constant across the eddy (data not shown). Pigment distributions in the water column indicate that the characteristic two-layer distribution (cyanobacteria in the mixed layer and small eukaryotes and *Prochlorococcus* spp. occupying the DCM) was not disrupted, but was merely displaced upwards by ~20 m.

Photosynthetic pigments were integrated to the 1% LL (110 m in and 115 m out of the eddy). Depth-integrated TChl *a* concentrations were relatively constant in and out of *Noah*, as were most pigment inventories (i.e. TChl *b*, TChl *c*, DDX, α-Car, β-Car, Zeax). However, the fraction of TChl *a* attributed to MVChl *a*, which is present in all phytoplankton, increased to ~60% in *Noah* compared to ~50% at OUT stations. In contrast, the fraction of TChl *a* attributed to DVChl *a* was ~42% versus ~50% outside of *Noah*. These fractions indicate that the dominance by *Prochlorococcus* spp. in ambient conditions shifted towards other types of phytoplankton in the eddy, such as diatoms (1.7-fold increase in Fuco), prymnesiophytes (~1.4-fold increase in Hex-fuco), pelagophytes (~1.3-fold increase in But-fuco), and dinoflagellates (~1.7-fold increase in Per). Allox, DTX, Pras, Viola, and the chlorophyll degradation pigment MVChld *a* were only present in trace amounts both in an out of *Noah*; hence, all but MVChld *a* (important in Cyclone *Opal*, Section 3.2.2) were omitted from Table 3.

3.1.3. *Phytoplankton size structure*

TChl *a* concentration did not change significantly at the base of the mixed layer in and out of *Noah* (Table 4). Within that layer, however, a modest shift in phytoplankton size structure to cells >18 μm is apparent (5.4% IN versus 2.8% OUT, Table 4). A ~1.3-fold increase in TChl *a* concentration was evident within the mixed layer of the center of the eddy, which was comprised mainly of picoplankton 0.7–2 μm (i.e. *Prochlorococcus* sp.) with modest increases in nanoplankton 2–18 μm such as pelagophytes and prymnesiophytes (15.0% IN compared to 11.3% OUT) and microplankton >18 μm such as diatoms (7.6% IN compared to 3.0% OUT).

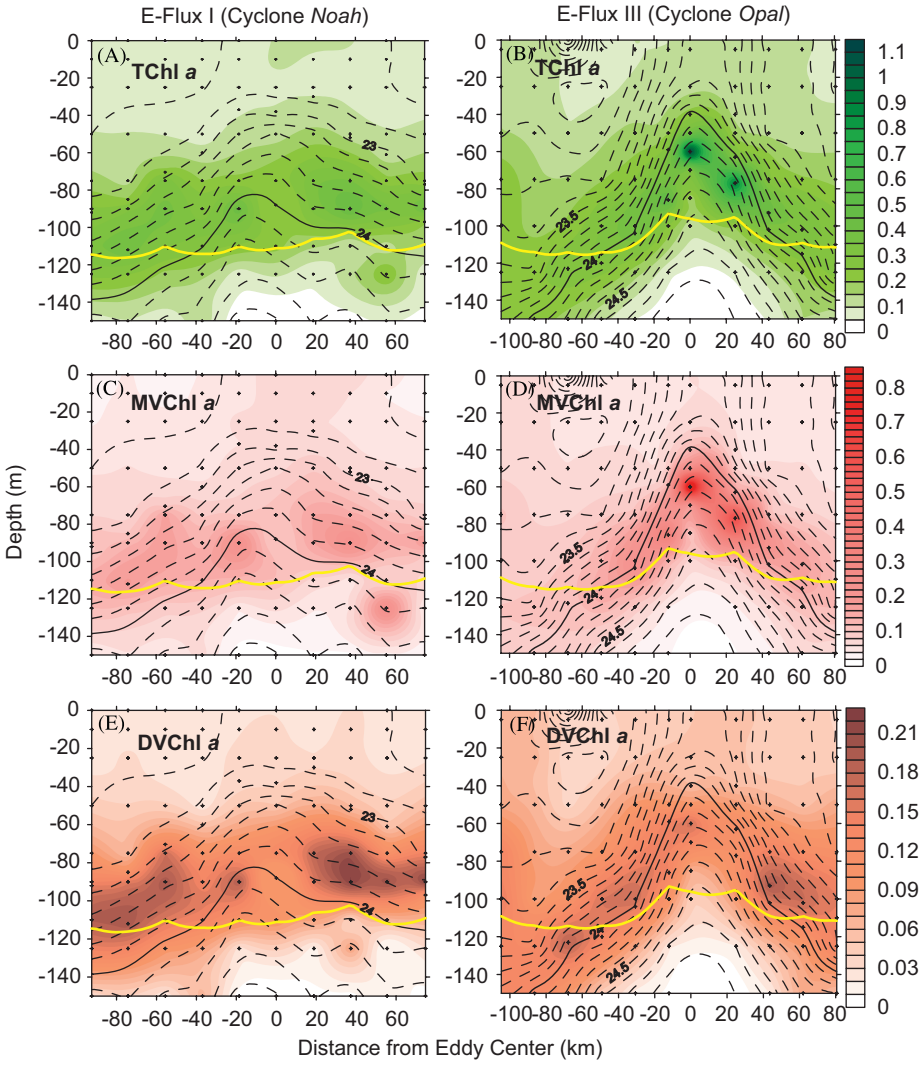

Fig. 4. Depth contours of chlorophyll pigment biomarkers from Transect 3: TChl *a* = MVChl *a*+DVChl *a*+MVChld *a* (mg m^{-3}, panels A, B), MVChl *a* (mg m^{-3}, panels C, D), and DVChl *a* (mg m^{-3}, panels E, F) in Cyclones *Noah* and *Opal*, with overlays of isopycnal surface contours and a yellow line representing the depths of the euphotic zone (1% surface LL). Crosses indicate sampling locations.

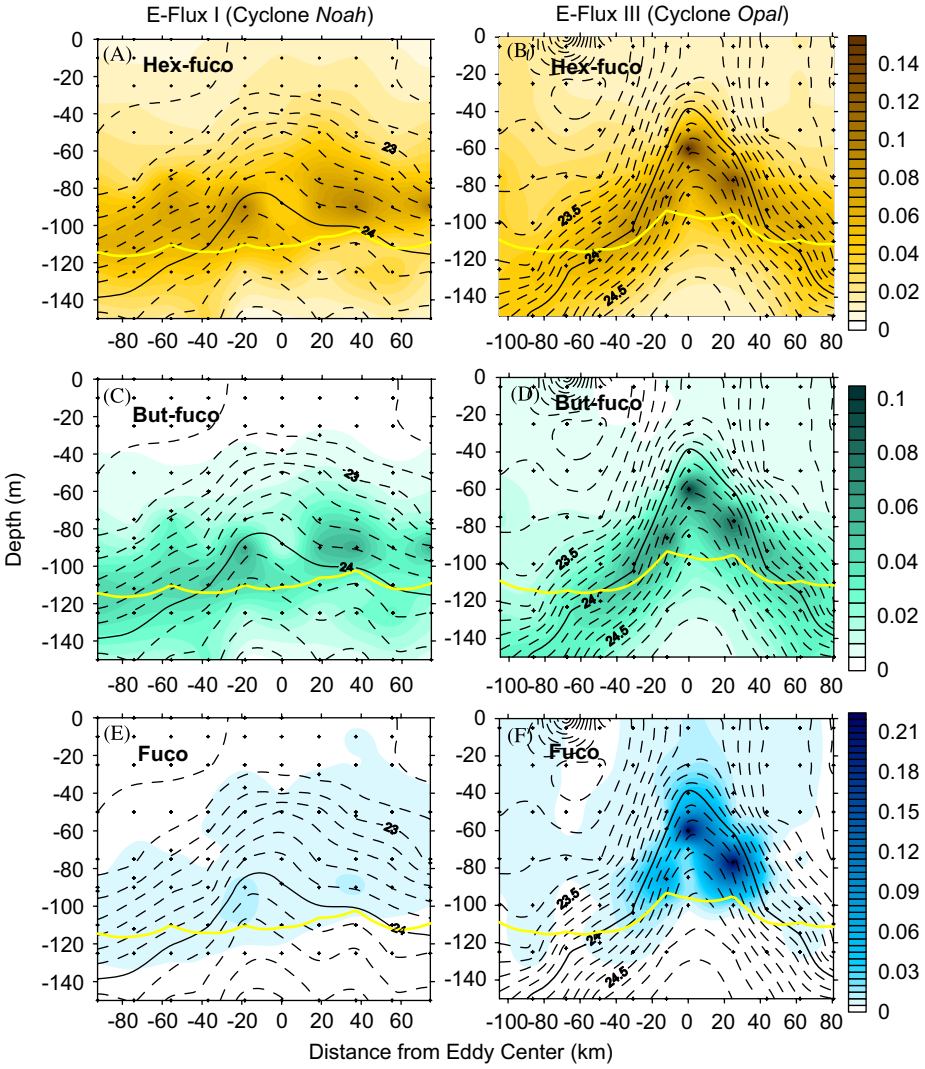

Fig. 5. Depth contours of carotenoid pigment biomarkers from Transect 3: Hex-fuco (mg m^{-3}, panels A, B), But-fuco (mg m^{-3}, panels C, D), and Fuco (mg m^{-3}, panels E, F) in Cyclones *Noah* and *Opal*, with overlays of isopycnal surface contours and a yellow line representing the depths of the euphotic zone (1% surface LL). Crosses indicate the depth of sampling at each station.

3.1.4. *Particulate matter export*

The sediment trap array remained within *Noah* for the entire duration of the deployment (drifter trajectories for E-Flux I are shown in Dickey et al., 2008). Particulate carbon, nitrogen, and silica exports were not significantly different in and out of *Noah* (Table 5). Exported TChl *a* was higher by ~1.2-fold in the eddy compared to out, with concurrent increases in exported pigments DTX and β-Car (data not shown). All other exported pigments within the eddy were ~30-50% less than those in surrounding waters.

3.2. *Cyclone Opal*

Cyclone *Opal* became visible in GOES and MODIS SST imagery on 18 February 2005, but likely formed below the surface prior to this date. *Opal* was approximately a month old at the time of our study (10–22 March 2005) with colder surface water evident in satellite imagery. Over our 3-week observation, *Opal* drifted ~165 km (88–89 nmi) southward from its original location (~20.3 °N, 156.3 °W) while maintaining its physical structure. *Opal* remained visible in satellite imagery until April 2005, ~2 months after it first appeared (Nencioli et al., 2008; Dickey et al., 2008).

At 160–180 km in diameter and with a maximum eddy uplift of 80–100 m, *Opal* was a stronger and larger eddy than *Noah* at the time of sampling. Near-surface tangential velocities of ~60 cm s^{-1} increased almost linearly from the center up to a radial distance of ~25 km. The angular velocity of ~2.4×10^{-5} rad s^{-1} (orbital period is ~3 days) remained nearly constant within the radial distance. This area of constant angular velocity indicates that this portion of the eddy was in near-solid-body rotation, relatively isolated from surrounding waters (Nencioli et al., 2008). The dimensions of *Opal* were inferred from hydrographic data; more detail regarding horizontal and vertical dimensions of the feature is described in Nencioli et al. (2008). Doming of isopycnals was markedly more intense in *Opal* than *Noah*, as evidenced by shoaling of the σ–$t_{24.0}$ density surface (52 ± 8 m IN, 131 ± 15 m OUT) and depth of the 1% LL (91 ± 11 m IN, $n = 45$; 112 ± 4 m OUT, $n = 21$). *Opal* was a relatively shallow feature as the cyclonic circulation was insignificant at depths greater than 200 m (Nencioli et al., 2008).

3.2.1. *Macronutrient distributions*

Similar to *Noah*, macronutrient concentrations reflected shoaling of isopycnal surfaces but were much more pronounced in *Opal* (Fig. 2). During the initial sampling of *Opal*, N+N was present in

Table 3
Depth-integrated photosynthetic pigments (mg m^{-3}) during E-Flux I (Cyclone *Noah*) and E-Flux III (Cyclone *Opal*)

	E-Flux I			E-Flux III		
	Cyclone *Noah*			Cyclone *Opal*		
	IN ($n=2$)	OUT ($n=3$)	IN/OUT	IN ($n=8$)	OUT ($n=3$)	IN/OUT
Chlorophylls (mg m^{-3})						
TChl *a*	22.75 (2.0)	18.99 (6.9)	1.2	27.68 (3.7)	18.95 (3.1)	1.5
MVChl *a*	13.16 (0.8)	9.50 (2.2)	1.4	18.20 (3.0)	9.97 (1.3)	1.8
DVChl *a*	9.53 (1.3)	9.43 (4.7)	1.0	7.46 (1.0)	8.78 (1.6)	0.8
MVChld *a*	0.05 (0.1)	0.05 (0.1)	1.0	2.10 (1.3)	0.21 (0.1)	10.0
TChl *b*	6.88 (0.8)	4.77 (2.5)	1.4	6.12 (1.4)	4.63 (1.2)	1.3
TChl *c*	4.97 (0.5)	3.51 (1.3)	1.4	7.89 (1.3)	3.35 (0.5)	2.3
Xanthophylls (mg m^{-3})						
But-fuco	2.28 (0.3)	1.71 (0.7)	1.3	2.69 (0.4)	1.54 (0.3)	1.7
DDX	0.54 (0)	0.41 (0.1)	1.3	1.01 (0.2)	0.70 (0)	1.4
Fuco	0.79 (0.1)	0.46 (0.1)	1.7	4.22 (1.4)	0.78 (0)	5.4
Hex-fuco	4.85 (0.3)	3.37 (1.2)	1.4	4.32 (0.5)	3.14 (0.6)	1.4
Per	0.50 (0.1)	0.30 (0.1)	1.7	0.51 (0.1)	0.33 (0.1)	1.5
Zeax	5.12 (0.5)	5.47 (1.6)	0.9	5.01 (0.4)	8.42 (0.6)	0.6
Carotenes (mg m^{-3})						
α-Car	2.02 (0.2)	1.72 (0.8)	1.2	1.70 (0.4)	2.05 (0.4)	0.8
β-Car	0.56 (0.0)	0.41 (0.1)	1.4	0.87 (0.3)	0.23 (0.1)	3.8

All pigments were depth-integrated to the depth of the euphotic zone (1% LL): *Noah* (110 m IN, 115 m OUT), *Opal* (100 m IN, 115 m OUT). Values in columns indicate mean ($\pm$s.d. or range). Mean values from E-Flux I: IN = IN Sta. 1–2, OUT = OUT Sta. 1–3; from E-Flux III: IN = Cast 19A and IN Sta. 1–7, OUT = OUT Sta. 1–3. Pigments that were detected but present in trace amounts (<0.2 mg m^{-3}, Allox, DTX, Pras, Viola) were omitted from the table.

Table 4
Size-fractionated TChl *a* in and out of Cyclones *Noah* and *Opal* within (43% LL) and at the base (11% LL) of the mixed layer (ML)

Depth (m)	% Light level	Location in mixed layer	Location in eddy	[TChl *a*] (mg m^{-3})	Size-fractionated [TChl *a*]		
					0.7–2 μm (% total)	2–18 μm (% total)	>18 μm (% total)
E-Flux I Cyclone Noah							
16	43	In ML	IN	90.6 (23)	77.5 (0.1)	15.0 (0.1)	7.6 (0.1)
20	43	In ML	OUT	69.9 (9)	85.7 (3.0)	11.3 (4.6)	3.0 (1.9)
39	11	Base of ML	IN	117.2 (9)	84.8 (0)	9.8 (0)	5.4 (0.4)
50	11	Base of ML	OUT	117.5 (12)	87.5 (1.1)	9.7 (2.3)	2.8 (1.2)
E-Flux III Cyclone Opal							
15	43	In ML	IN	120.9 (6)	81.6 (1.7)	13.3 (0.9)	5.1 (0.9)
20	43	In ML	OUT	88.5 (11)	85.1 (0.5)	11.6 (0.6)	3.3 (1.1)
35	11	Base of ML	IN	175.3 (47)	70.5 (11)	21.0 (8.6)	8.5 (2.9)
55	11	Base of ML	OUT	129.7 (13)	88.8 (0.5)	9.1 (0.9)	2.0 (0.3)

Size-fractionated TChl *a* is presented as a percentage of the total TChl *a*. Values in columns indicate mean ($\pm$s.d. or range) taken from IN Sta. 1–3 ($n=3$) and OUT Sta. 1–2 ($n=3$) for Cyclone *Noah*, and from IN Sta. 1, 3, 4 ($n=3$) and OUT Sta. 1–2 ($n=2$) for Cyclone *Opal*.

Table 5
Particulate export fluxes ($\pm$s.d.) obtained using a sediment trap array deployed in ($n=3$) and out ($n=3$) of Cyclones *Noah* and *Opal*

Parameter	IN	OUT	ANOVA[a]	IN/OUT
Particulate biogenic silica (mmol Si m^{-2} d^{-1})				
Noah	0.12 (0.04)	0.10 (0.0)	$p=0.5$ NO	1.2
Opal	0.43 (0.03)	0.11 (0.06)	$p=0.002$ YES	3.9
Particulate carbon (mmol C m^{-2} d^{-1})				
Noah	2.20 (0.2)	2.31 (0.3)	$p=0.6$ NO	1.0
Opal	1.54 (0.1)	1.52 (0.2)	$p=0.9$ NO	1.0
Particulate nitrogen (mmol N m^{-2} d^{-1})				
Noah	0.24 (0.03)	0.27 (0.03)	$p=0.5$ NO	0.9
Opal	0.15 (0.01)	0.16 (0.02)	$p=0.3$ NO	0.9
Particulate phosphorus (μmol P m^{-2} d^{-1})				
Noah	2.57 (0.3)	4.28 (0.7)	$p=0.02$ YES	0.6
Opal	2.69 (1.0)	2.07 (1.1)	$p=0.5$ NO	1.3

[a] Single-factor analysis of variance tested whether the means are significantly different from one another with 95% confidence.

trace amounts ($\geqslant$ the limit of detection) above the σ–$t_{24.0}$ density surface, whereas silicic acid concentration was below detection limits within a confined area (~20 km) in the center of the eddy along the σ-$t_{24.0}$ isopycnal surface (depth ~40–60 m). All three contour plots of N+N, phosphate, and silicic acid show penetration of deep water nutrients into the euphotic zone (indicated by the yellow line) in the center of *Opal* (Fig. 2).

Increases in N+N, phosphate, and silicic acid concentrations integrated over 0–150 m compared to surrounding waters were 4.1-, 1.8-, and 1.1-fold, respectively (Table 2). When integrated over the euphotic zone (0-100 m IN, 0-115 m OUT), the values indicated less enhancement in N+N (2.7-fold) and phosphate (1.4-fold) and a slight decrease in silicic acid (0.9-fold) which may be negligible when taking into account the high standard deviation ($\pm$25 for both IN and OUT stations).

3.2.2. Photosynthetic pigment biomarkers

Depth profiles of TChl *a* in the center showed a sharp and dramatic increase within *Opal*, as indicated by a ~50 m upward

displacement and a marked >2-fold increase at the DCM (Fig. 3B). The depth of the DCM at IN stations varied dramatically during our study though the DCM was confined within a narrow band of isopycnal surfaces $\sigma{-}t_{24.2}$ ($\sigma_t = 24.2\,\mathrm{kg\,m^{-3}}$) and $\sigma{-}t_{24.4}$ ($\sigma_t = 24.4\,\mathrm{kg\,m^{-3}}$) (Fig. 3C). The DCM in the eddy occupied a denser isopycnal surface ($\sigma{-}t_{24.3}$, $\sigma_t = 24.3\,\mathrm{kg\,m^{-3}}$) than the DCM in surrounding waters ($\sigma{-}t_{23.8} = 23.8\,\mathrm{kg\,m^{-3}}$; Fig. 3C). The TChl *a* bloom was comprised mostly of phytoplankton containing MVChl *a* (Fig. 4D) and pigments Hex-fuco, But-fuco, and Fuco (Fig. 5). Most notably, Fuco exhibited a ~60-fold increase in the DCM in the center of *Opal* relative to ambient waters. *Prochlorococcus* spp. (DVChl *a*) did not appear to contribute to the bloom, as the highest DVChl *a* concentrations were observed at the periphery of the center (Fig. 4F). Similarly to *Noah*, the cyanobacterial pigment Zeax was present primarily in the mixed layer above the $\sigma{-}t_{24.0}$ density surface (data not shown). Zeax concentration did not change across the eddy, again suggesting that eddy processes do not disrupt the characteristic two-layer distribution but merely displace populations upwards by ~50 m.

Euphotic zone integrated TChl *a* concentrations indicated a 1.5-fold increase in *Opal* compared to out (Table 3). MVChl *a* comprised 66% of the TChl *a* concentration in the eddy as compared to 52% out, while the DVChl *a* fraction in *Opal* was only 27% compared to 47% out of *Opal*. These fractions are a clear indication of the shift in phytoplankton community from *Prochlorococcus* spp. dominance to eukaryotic phytoplankton in the eddy. The remaining fraction (7%) of TChl *a* in *Opal* was made up of the chlorophyll degradation pigment MVChld *a*, which typically represents the presence of senescent diatom cells or zooplankton fecal pellets. This marked increase in MVChld *a* concentration in *Opal* is attributed to senescent diatom cells concurrent with a 5.4-fold increase in Fuco in *Opal* compared to out. Modest enhancements of other eukaryotic phytoplankton, such as pelagophytes (1.7-fold increase in But-fuco) and prymnesiophytes (1.4-fold increase in Hex-fuco) were also observed, as were increases in TChl *c*. In contrast, cyanobacterial pigments DVChl *a*, Zeax, and α-Car were observed to be slightly depressed, indicating altered community dynamics in *Opal*'s center.

3.2.3. Phytoplankton size structure

A 1.4-fold increase in TChl *a* concentration was evident at the base of and within the mixed layer in *Opal*. The phytoplankton community at the base of the mixed layer in *Opal* had fewer 0.7–2 μm cells than out (70.5% IN and 88.8% OUT), but considerably higher number of cells in the 2–18 μm and >18 μm size classes (Table 4). In the mixed layer community, there were slight increases in the proportion of phytoplankton ⩾2 μm, but a slight decrease in phytoplankton ⩽2 μm. Greater than 50% of the total Fuco concentration in the DCM was due to diatoms >18 μm, as determined by size-fractionated HPLC (data not shown). In Transect 6, the concentration of size-fractionated Fuco decreased dramatically while DVChl *a* displayed a modest increase from the center towards the edge of the eddy.

3.2.4. Time series in Opal center

Tracking *Opal* and the location of the center proved to be challenging. As outlined in Section 2.1, extensive analyses of satellite, ship-based, and drifter observations were utilized to ensure sampling of the center during our time series. Near real-time ADCP velocities, combined with underway *in situ* temperature, proved to be the most useful tool in tracking the center and permitted real-time modifications of the original sampling pattern. Data was then treated as quasi-synoptic when plotted and interpreted with respect to the moving center of the eddy in a quasi-Lagrangian reference frame. Trajectories of the OPL drifter, the METOCEAN bio-optical drifter, and the sediment trap array were analyzed post-cruise to locate the geometric centers of the trajectories for comparison with the sampled 'centers' of the eddy. Further information concerning the center of *Opal* was inferred from the analyses of the distributions of the differential anomalies of temperature and density. All of the above methods indicate that we were able to sample the 'center' of *Opal*. Nencioli et al. (2008) detail the post-cruise analyses on the physical aspects of *Opal* and the quasi-Lagrangian framework of sampling, validating a time series in the 'center' of *Opal*.

The phytoplankton community in the center of *Opal* evolved substantially over the 8-day time series (Fig. 6). The center station (cast 19A) during transect 3 was included in this time series as t_0 ($t = 0$ h) such that the gap between t_0 and IN Station 1 ($t_1 = 58$ h) represents lack of data, not lack of pigment. From t_0 to t_1, the DCM deepened in the water column from ~50–70 m to 70–90 m, and then varied considerably during consecutive days. The variability in DCM depth may be attributed to ship positioning, eddy dynamics, internal tides, or inertial variability, which has

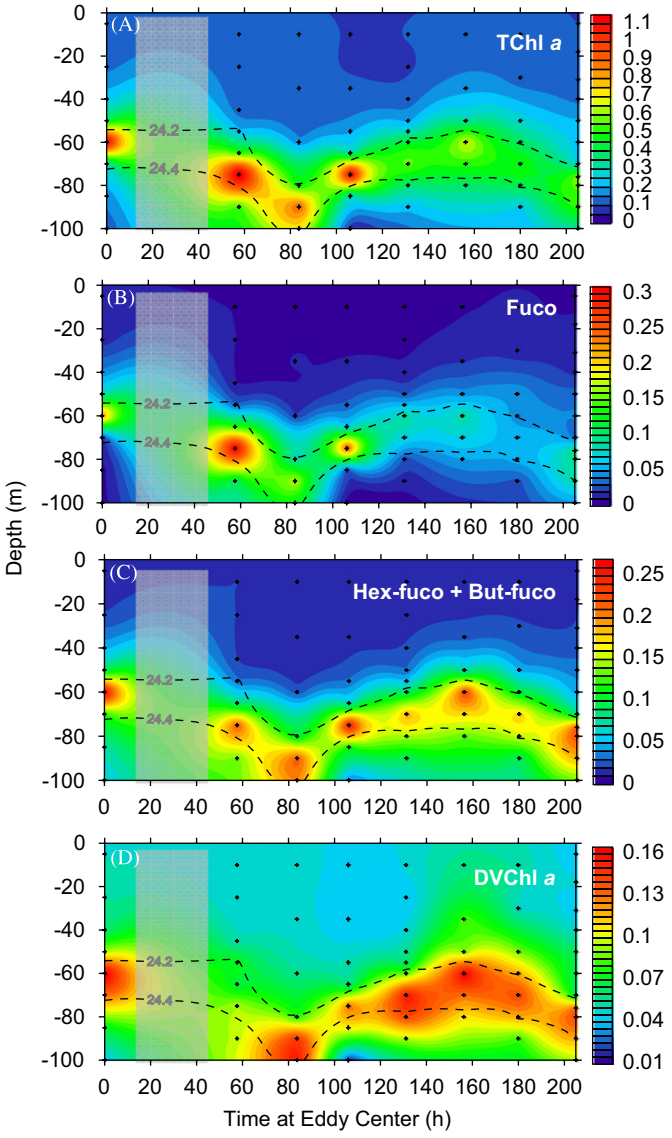

Fig. 6. Eight-day time series of photosynthetic pigments at the Cyclone *Opal* center (casts 19A, IN stations 1–7): TChl *a* ($\mathrm{mg\,m^{-3}}$, A), Fuco ($\mathrm{mg\,m^{-3}}$, B), Hex-fuco+But-fuco ($\mathrm{mg\,m^{-3}}$, C), and DVChl *a* ($\mathrm{mg\,m^{-3}}$, D). Crosses indicate depths of sampling at each station. Dashed lines indicate the location of isopycnal surfaces $\sigma{-}t_{24.2}$ and $\sigma{-}t_{24.4}$ and the gray box indicates the period of no data.

a ~31-h periodicity (Karl et al., 2002). Despite the variability, the DCM remained narrowly confined within isopycnal surfaces $\sigma-t_{24.2}$ and $\sigma-t_{24.4}$ (as indicated by dotted lines, Fig. 6), implying that sampling occurred in the same water mass. Within this layer, TChl *a* concentration decreased dramatically after 4 days to half its original concentration (from ~1.1 to 0.5 mg m^{-3}, Fig. 6A). The decline of the bloom was largely due to the decrease in diatoms, as indicated by Fuco (Fig. 6B). But-fuco and Hex-fuco maintained the same elevated concentration throughout the 8 days in the center of *Opal*, representing a persistent bloom dominated by pelagophytes and prymnesiophytes (Fig. 6C). DVChl *a* also remained constant over time, representing the ambient population of *Prochlorococcus* spp. (Fig. 6D).

3.2.5. Suspended biogenic silica profiles

A single profile of suspended BSi was obtained both in (IN Sta. 2) and out (OUT Sta. 3) of *Opal* (Fig. 7). The BSi maximum was displaced upwards from ~120 m in the surrounding waters to ~45 m within the eddy center with a ~20-fold increase compared to ambient BSi concentrations.

3.2.6. Particulate matter export

The sediment trap array remained within *Opal* as it traveled southward during the study (drifter tracks are shown in Dickey et al., 2008). Particulate carbon and nitrogen export was similar in and out of the eddy, but particulate silica export was ~4-fold higher at the eddy center (Table 5). Microscopic examination of trap solution from out of Cyclone *Opal* showed little material whereas samples collected within *Opal* contained nearly empty frustules of large diatoms. Increased silica export within the eddy was likely due to the export of such frustules, which contained little visible chlorophyll or cellular organic material.

Exported TChl *a* was ~1.3-fold higher in *Opal* compared to out (data not shown). An associated increase in exported MVChl *a* from inside *Opal* was concurrent with a ~1.5-fold increase in exported Fuco, with noticeable increases in Pras, DTX, and DDX relative to out of *Opal*. Exported Zeax was greater out of the eddy by ~1.5-fold. Surprisingly, exported But-fuco, Hex-fuco, and Per were also higher (~2-fold) out of the eddy, indicating greater export of smaller pelagophytes, prymnesiophytes, and dinoflagellates from the water column out of *Opal*.

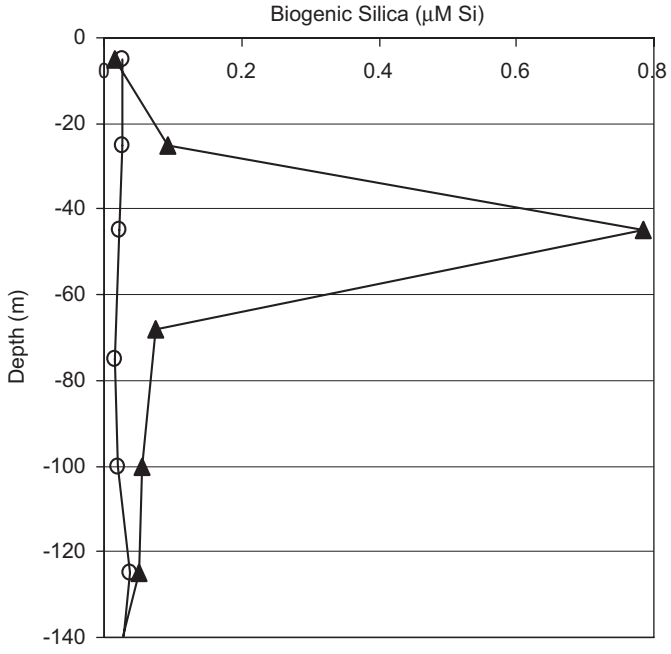

Fig. 7. Depth profile of suspended biogenic silica from IN Sta. 2 (closed triangles) and OUT Sta. 3 (open circles) for Cyclone *Opal*.

4. Discussion

4.1. The transient oasis

The uniqueness of Cyclone *Opal* is highlighted by the presence of large, chain-forming diatoms, which was unexpected given previous findings (Olaizola et al., 1993; Seki et al., 2001; Bidigare et al., 2003; Vaillancourt et al., 2003). In addition to significant increases in diatom biomass (indicated by Fuco concentration), Brown et al. (2008) observed a 100-fold increase in >20 μm diatom biomass as measured using microscopy at 70–90 m in the center of *Opal*. The sudden decline of the diatom bloom after our fourth day in the center of *Opal* emphasizes the importance of timing in the sampling of mesoscale eddy features in the open ocean. It is difficult to estimate the duration of the bloom, for it most likely began prior to our arrival. The decay of the diatom bloom may have been the result of several biological processes, including grazing pressure, interspecies competition, as well as viral infection. After close examination of our data, we attribute physiological stress due to Si limitation as a probable cause of the demise of the diatom bloom.

Si is essential for the formation of diatom frustules (Guillard, 1975; Brzezinski and Nelson, 1996). The strongest evidence for Si limitation, given that direct uptake experiments were not performed in this study, was silicic acid depletion (⩽limit of detection) at ~40–60 m in the center of *Opal* in Transect 3. These depths contained the DCM and a 60-fold increase in Fuco. It has been reported that ambient silicic acid concentrations of ⩽1–2 μM limit uptake by diatoms in surface waters of most mid-ocean gyres (Egge and Aksnes, 1992; Brzezinski and Nelson, 1995, 1996; Brzezinski et al., 1998, 2001; Henson et al., 2006). Silicic acid levels during E-Flux III were correlated with density surfaces and were found to be <2 μM in the euphotic zone in *Opal* (Fig. 8B); these levels likely limited silicic acid uptake by diatoms. In contrast, silicic acid concentrations in *Noah* ranged from 0 to 3 μM (Fig. 8A) and did not seem to limit uptake by phytoplankton, as the phytoplankton community within *Noah* was dominated by non-diatom phytoplankton that do not require Si for growth.

Although low concentrations do not prove nutrient limitation, diatoms in *Opal* did show signs of physiological stress. High levels of MVChld *a*, indicative of senescent phytoplankton and fecal pellets, were measured in the DCM concurrent with a 60-fold increase in Fuco pigment. Landry et al. (2008) reported depressed growth rates and a higher biomass of physiologically unhealthy diatoms in the 50–60 m depth zone, while healthy diatoms were observed immediately below at the base of the euphotic zone (70–90 m). Brown et al. (2008) observed a similar phenomenon in which a distinct layer of senescent diatoms were present in these upper depths while healthier diatoms were present directly below. All of the above, plus the lack of phytoplankton response to N, P, and Fe additions in the eddy, point to Si limitation as the primary cause of the decline in diatom biomass (Benitez-Nelson et al., 2008).

If Si limitation indeed accounts for the decline of the diatom population, depletion of Si would then lead to utilization of the "next" limiting nutrient, for only one essential nutrient can limit growth rate at a specific time (Tilman, 1980). After the demise of the diatom bloom, the sustained background population of smaller eukaryotes and cyanobacteria was maintained by sufficient N and P remaining within Cyclone *Opal*. This would suggest that the "apparent" succession of large Si-dependent diatoms by

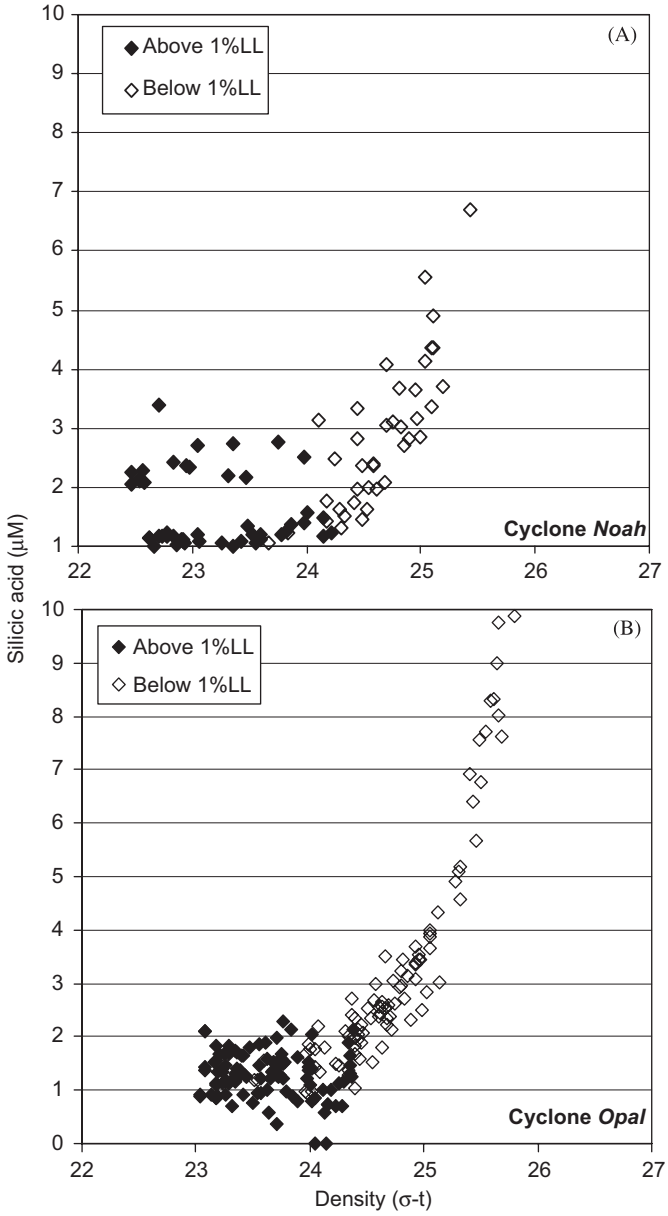

Fig. 8. Scatterplots of silicic acid against density from all samples (Transect 3 and process stations) from E-Flux I (Cyclone *Noah*, panel A) and E-Flux III (Cyclone *Opal*, panel B): silicic acid concentrations in the euphotic zone (above 1% LL, closed diamonds) and below the euphotic zone (below 1% LL, open diamonds) are specified.

pico- and nano-phytoplankton (*Prochlorococcus* spp., pelagophytes, prymnesiophytes, and other lightly silicified diatoms), as observed during the time series in the *Opal* center was primarily caused by nutrient limitation. It is likely that phytoplankton with high maximum nutrient uptake rates (V_{max}) (i.e. diatoms), in their unhealthy state, may be outcompeted by those with lower V_{max} (i.e. prymnesiophytes and pelagophytes), ultimately altering phytoplankton community dynamics. Similar changes in phytoplankton community structure have been observed during a North Atlantic spring bloom event, when diatoms were outcompeted by non-siliceous phytoplankton upon silicic acid depletion (Henson et al., 2006). Even though diatoms require Si to form frustules, several species such as *Hemiaulus* and *Mastogloia* spp. produce thinner frustules (Brzezinski and Nelson, 1996; Scharek et al., 1999a) under substrate limitation. These lightly silicified species were observed at the end of the time series in Cyclone *Opal* (Benitez-Nelson et al., 2008; Brown et al., 2008).

Presumably, once Si becomes limiting to diatom growth, production by non-siliceous phytoplankton would continue until all remaining N or P has been consumed. However, Henson et al. (2006) showed that although Si may limit a bloom and by extension export production, subsequent utilization of N or P serves to ultimately restore conditions towards production by recycling nutrients. Once N reaches a minimum value, all further production must rely on recycled forms of N (Henson et al., 2006), suggesting that phytoplankton in the 'decay' stage of a cyclonic eddy would ideally return to regenerated production. Mahaffey et al. (2008) reported that suspended particulate N was markedly enhanced in the DCM within *Opal*, possibly due to small fecal pellets and/or organic matter that had yet to be exported. Mixed-layer depth-integrated values of particulate N decreased significantly during the time series at the *Opal* center, indicating either remineralization or export of N. However, increases in inorganic N (nitrate, nitrite) or N export flux was not observed, indicating a shift towards recycled production (via NH_4^+ assimilation) and/or new production via nitrogen fixation as the primary means of N supply.

4.2. Subtropical eddies: a silica pump?

Enhanced biological activity and a shift up in size structure of the phytoplankton community are thought to stimulate rates of carbon export (McCave, 1975; Eppley and Peterson, 1979; Knauer et al., 1979; Goldman, 1988, 1993). Given modest increases in photosynthetic pigment biomass, it is not surprising that export fluxes in *Noah* did not exhibit significant differences from ambient waters. Despite variability in phytoplankton populations in *Opal*, the presence of large diatoms had foreshadowed enhanced rates of carbon export. Several biases are associated with sediment trap use, such as hydrodynamic flow above the trap mouth and over- or underestimation of organic carbon attached to swimmers accidentally caught in trap tubes (Butman et al., 1986; Buesseler, 1991; Buesseler et al., 2000). However, only a modest 1.3-fold increase in ^{234}Th-derived carbon flux (Benitez-Nelson et al., 2008; Maiti et al., 2008) was observed, corresponding to the trap-derived export estimates in the center of *Opal*. It can be argued that we may have missed the timely carbon export event of *Opal*, but this is unlikely. Mass balance estimates suggest that >85% of net community production accumulated as total organic carbon (comprised mostly of dissolved organic carbon) within the system (Benitez-Nelson et al., 2008), consistent with the minimal carbon export evidenced in traps and in ^{234}Th- and ^{210}Po-derived measurements. Hence, most of the carbon generated within *Opal* was remineralized rather than exported (Maiti et al., 2008; Verdeny et al., 2008). We suspect that the major export event consisted primarily of BSi, as observed in the form of empty diatom frustules in the sediment trap array. In addition, high levels of suspended BSi were observed at ~50 m (Fig. 7), likely due to large and spiny senescent diatoms with slow sinking rates, such as *Chaetoceros* spp. (Brown et al., 2008). Furthermore, these results suggest that cyclonic eddies formed in subtropical waters may not necessarily be an efficient mechanism for exporting particulate carbon to the mesopelagic zone. This finding is consistent with a recent temperature-dependent food web model that predicts low carbon export efficiencies in waters with surface temperatures exceeding 25 °C, as is the SNPO (Laws et al., 2000; Benitez-Nelson et al., 2008). The absence of a major carbon flux event is likely due to strong microbial community coupling of production, microzooplankton grazing (Landry et al., 2008), and thus remineralization processes. In the case of *Opal*, minimal

carbon flux was replaced by a large BSi flux (~4-fold higher than out of the eddy). Subtropical cyclonic eddies must now be re-evaluated as potential silica pumps, suggesting that phytoplankton in the SNPO will be limited by Si following a major eddy event (Benitez-Nelson et al., 2008).

4.3. Noah vs. Opal

Based on the age model of Sweeney et al. (2003), Cyclones *Noah* and *Opal* represent two out of three stages in a cyclonic eddy's biological life cycle. Physical data (Kuwahara et al., 2008) as well as nutrient inventories and photosynthetic pigment distributions suggest that *Noah*, ~3 months old, was in the 'decay' stage. *Opal*, a month old at the time of encounter, appeared to be 'mature' but began to 'decay' biologically while it remained physically 'mature' (Nencioli et al., 2008). If we follow the biological life cycle model, it is feasible to presume that *Noah* had contained a diatom bloom in its 'mature' stage like in *Opal*, and would then exhibit signals of enhanced export in its 'decay' stage. However, enhanced carbon export was not observed in either eddy in our study. Nencioli et al. (2008) hypothesized that *Opal* was a unique case in which its fast southward translation during our observational period resulted in radial movements of water between the center and outer portions along the upper density surfaces. They inferred an exchange between waters at 70–90 m in the center portion and waters at 130–150 m in the peripheral portion, along the isopycnal surfaces of $\sigma{-}t_{23.6}$ and $\sigma{-}t_{24.4}$. This 'open-bottom/horizontally leaky' eddy hypothesis provided additional injections of nutrients along the path of propagation, leaving a wake of TChl *a* biomass behind. Thus, the eddy's translation speed and velocity field may significantly affect the system in terms of open or closed, and in turn, its productivity. However, given that the upper water column (100–130 m) of *Opal* was reported to be in solid body rotation (Nencioli et al., 2008), the above hypothesis explains neither the unique phytoplankton community in *Opal* nor previously studied eddies. A closer look at recently studied cyclones *Mikalele*, *Loretta*, and *Haulani* (Seki et al., 2001; Bidigare et al., 2003) provides several insights.

Cyclones *Mikalele* and *Loretta* (Seki et al., 2001) were ~1 and 6 months old, respectively. During observation, *Mikalele*, a small eddy (~100 km) that was speculated to be 'intensifying,' expressed strong surface thermal gradients and a ~1.5-fold increase in Fuco and Hex-fuco. *Loretta*, also ~100 km in diameter, appeared to be in its 'decay' stage at the time of observation and had been a cohesive eddy for ~6 months, yet still displayed significant ~2-fold increases in Fuco, But-fuco, and Hex-fuco, with outcroppings of isopycnal surfaces resembling that of *Opal* (Seki et al., 2001). *Loretta* maintained a bloom of prymnesiophytes and pelagophytes even after 6 months. How was *Loretta* able to maintain a bloom for so long when *Opal* illustrated a classic 'bloom and bust' scenario? Why did *Mikalele* and *Opal*, both 1 month old, support such different communities of phytoplankton?

Further confounding interpretations, Cyclone *Haulani* exhibited a ~25-fold increase in prymnesiophytes (mostly coccolithophores) and an increase in small, pennate diatoms (Vaillancourt et al., 2003). At 2 months old (like *Noah*), *Haulani*'s shape alternated between circular and elliptical within the first month, possibly due to variability in wind strength. *Haulani* was the only cyclone studied to date that exhibited a ~2.6-fold increase in carbon export, albeit the absolute magnitude was still low (Bidigare et al., 2003). Moreover, *Haulani* remained visible in satellite imagery for 3 months after observation, implying that *Haulani* may not have been in a 'decay' phase at the time of enhanced carbon export. These inconsistencies raise the question of whether discrepancies in the biological responses of these cyclones are indeed due to age variability.

There are various other factors to consider in explaining cyclonic variability, such as sampling resolution, validity of OUT or control stations, coastal water entrainment, trace metal effects, grazing dynamics, and the possibility of cyclones born from different water masses (see Brown et al., 2008; Landry et al., 2008; Nencioli et al., 2008; Noble et al., 2008). The average lifespan of Hawaiian lee cyclones is between 3 and 8 months, significantly shorter than that of anticyclones, which propagate farther, generally spin more slowly and often last for over a year (Patzert, 1969; Lumpkin, 1998), or of eddies in the northwest Atlantic Ocean, which spin up as a result of baroclinic instability with a lifespan of at least 6 months (i.e. McGillicuddy and Robinson, 1997; Garçon et al., 2001; Flierl and McGillicuddy, 2002; Sweeney et al., 2003; McGillicuddy et al., 2007). Thus it can be hypothesized that anticyclones (and Sargasso Sea eddies) outlive cyclones due to slower spinning speed or because they are generally weaker in strength. Patzert (1969) distinguished between 'strong' and 'weak' eddies based on spin-up duration: a 'weak' eddy takes 1–2 weeks to spin up, while a 'strong' eddy requires 30 days or more. If so, 'strong' eddies may differ from 'weak' eddies in terms of biological response. Hence, spin-up duration may directly influence the type of bloom in a cyclone and consequently, the export flux.

'Spin-up duration' first must be properly defined. It can be characterized as: (1) the duration of upward flux of nutrients in the 'intensification' stage, or (2) the duration before which the potential energy of an eddy is directly proportional to the doming of the density structure (Patzert, 1969). In this study, the definition of 'spin-up duration' is simply the time period over which isopycnal surfaces are upwardly displaced into the euphotic zone, introducing nutrients into well-lit waters. Therefore, spin-up rate, or the rate of nutrient input into the euphotic zone, is dependent on wind velocity, direction, eddy shear dynamics, and circulation dynamics.

If spin-up rate does influence the type of phytoplankton bloom and subsequent export within a Hawaiian lee cyclonic eddy, then the dynamic between phytoplankton community structure and the rate of nutrient input is relevant. In reference to the paradoxical nature of closely competing phytoplankton species co-existing in a uniform body of water (Hutchinson, 1961), this co-existence is thought to occur primarily via limitation by different essential nutrients (Petersen, 1975): e.g., as Si limits diatom growth, N may limit growth of some diatoms as well as other phytoplankton, etc. In this case, a single varying nutrient concentration could lead to a shift in phytoplankton dominance (Eppley, 1969), and differences in nutrient supply could also lead to the dominance of specific phytoplankton (Turpin and Harrison, 1979). Linear features such as Rossby waves uplift isopycnals into a well-lit zone continuously in their line of propagation. Though the time-scale for the residence of a constantly propagating Rossby wave is relatively short, the nutrient input in a given passage area is relatively slow and constant. Thus, haptophytes and pelagophytes flourish because seed populations are abundant and smaller organisms are able to exploit excess (but less amounts of) N (Siegel, 2001; Uz et al., 2001; Sakamoto et al., 2004). In nonlinear features such as cyclonic eddies, faster input of nutrients or a single large addition into surface waters of a cyclone due to strong winds would provide an advantage to phytoplankton with high V_{max} (diatoms) over those with lower V_{max} (prymnesiophytes and pelagophytes) (also see Brown et al., 2008). An intense diatom bloom would be quickly limited by Si limitation and result in a 'bloom and bust' scenario, followed by a shift in phytoplankton community structure (Fig. 9A). Without a substantial increase in grazing by large zooplankton, remineralization would lead to opal-based export rather than carbon. However, slower input of nutrients due to weaker but longer

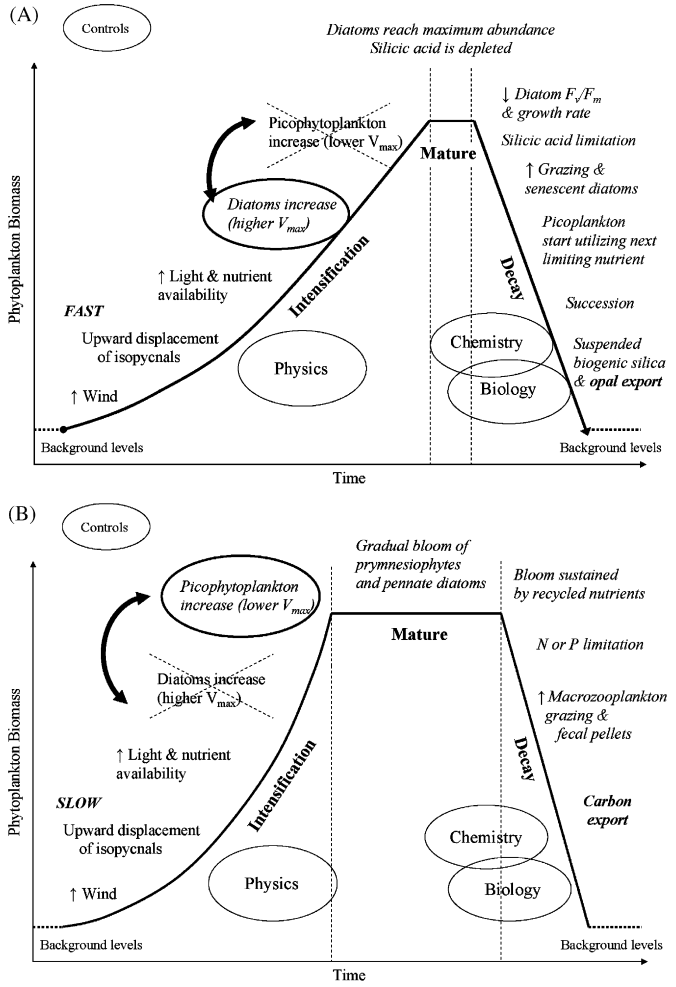

Fig. 9. Cartoon schematics of various types of controls on the biological life cycle of a cyclonic eddy in response to faster input of nutrients (panel A) and slower nutrient input (panel B).

duration of winds would favor a sustained bloom of carbon-rich phytoplankton such as prymnesiophytes (coccolithophores), altered food web dynamics, and an increase in macrozooplankton grazing. As a result, there would be an increase in organic carbon exported as fecal pellets into the mesopelagic zone (Fig. 9B).

The two scenarios are illustrated by the Hawaiian lee cyclones studied to date. The fast 'spin-up rate' scenario describes Cyclone *Opal*, with an abundance of large diatoms and significant opal export. Furthermore, Landry et al. (2008) reported a biologically stratified water column, in which the upper mixed zone (0–40 m) within *Opal* exhibited little biomass response, but significant increases in growth, grazing, and production of the ambient community, while the lower euphotic zone (70–90 m) was dominated by low growth rates but high biomass of large diatoms. The stratification may have been the result of slow nutrient input (in the upper mixed zone) and faster nutrient input (in the lower euphotic zone), indicating that spin-up rate could further dictate the depth structure of the plankton community within a cyclone.

The slow 'spin-up rate' scenario describes *Haulani*, with enhanced carbon export due to inorganic carbon ($CaCO_3$) contained within coccolithophores, a commonly found prymnesiophyte in the subtropical North Pacific. In fact, coccolithophores dominated the 25-fold increase in prymnesiophyte biomass within *Haulani* (Vaillancourt et al., 2003). It is also important to note that *Loretta* moved northwestward quickly after formation (Seki et al., 2001). Though its translation speed and eddy velocity field is not known, we can speculate that *Loretta* may have also been an 'open-bottom/horizontally leaky' eddy (Nencioli et al., 2008), indicating that its 6-month long bloom was sustained by a continuous injection of nutrients. According to the 'spin-up rate' hypothesis, a continuous nutrient input over a period of 6 months would indeed sustain a bloom of smaller eukaryotes. Therefore, this 'spin-up rate' hypothesis attempts to explain (1) *Opal*'s large centric diatom 'bloom and bust' occurrence and increased silica export, (2) the enhanced rate of carbon flux associated with increased coccolithophores in *Haulani*, and (3) *Loretta*'s 6-month-long sustained bloom.

In the case of *Opal* as an 'open-bottom/horizontally leaky' eddy (Nencioli et al., 2008), the 'spin-up rate' hypothesis still holds in the upper euphotic zone where phytoplankton with high V_{max} (diatoms) would have outcompeted those with lower V_{max} (prymnesiophytes and pelagophytes) after a single large nutrient addition. Perhaps the succession of phytoplankton from diatoms to smaller eukaryotes observed at the end of the time series in *Opal* can be attributed to continuous nutrient input into the center and peripheral portions of *Opal* due to the 'open-bottom,' similar to a Rossby wave. Nevertheless, these hypotheses emphasize the uniqueness of *Opal*: size, movement, community structure, and lack of expected carbon export.

Sweeney et al. (2003) briefly discussed the relevance of their conceptual model in terms of an eddy's age, intensity, and nutrient injection (i.e. single, multiple, consecutive). For eddies in the northwest Atlantic, which are significantly influenced by seasonal cycles, the 'spin-up' hypothesis becomes more complex in that the 'spin-up rate' of a Sargasso Sea eddy may be directly related to factors other than those in the SNPO. Correlations with 'spin-up rate' and the biological responses of previously studied eddies in the Sargasso Sea would allow further development and a broader application of this hypothesis. Quantitative measurements of 'spin-up rate' as well as numerical models of production determined by 'spin-up rate' would provide further insight into investigating the various hypotheses presented here.

5. Summary and conclusions

The two cyclones observed during this study, *Noah* and *Opal*, differed in terms of physical and biogeochemical attributes. Both eddies supported very different plankton communities in response to similar enhancements in standing stocks of macronutrients. While *Noah* exhibited only modest enhancements of the ambient phytoplankton community (dominated by *Prochlorococcus* spp. and small eukaryotes), *Opal* displayed a phytoplankton bloom dominated primarily by large diatoms in the DCM. The diatom-dominated bloom in *Opal* declined dramatically (as represented by a 50% decrease in Fuco) on the fourth day of our study period, likely due to Si limitation. Despite the presence of a large phytoplankton bloom, enhanced export of carbon or nitrogen was not observed in *Opal* (or in *Noah*); instead, a 4-fold increase in silica export (attributed to empty diatom frustrules) was observed in *Opal*. Therefore, it is likely that remineralization remained the key process within both eddy systems, despite enhancements in photosynthetic pigment biomass.

Previously, differences between cyclones have been attributed to the developmental stages of cyclonic eddies; however, characteristics of each eddy and its associated "age" are not in accordance. The characterization of *Noah* in the 'decay' stage and *Opal* as 'mature' implies that *Noah* once contained large diatoms similar to that observed in *Opal*. In addition, only one eddy in the past, *Haulani*, showed an enhancement in carbon export and the absolute magnitude was still low. Thus, we hypothesize that Hawaiian lee cyclones may follow different paths of development

stemming from differences in the 'intensification' stage. These differences may include wind strength, intensity of upwelling, eddy translation speeds, prior eddy activity in the area, and tangential velocity, all of which govern the rate of nutrient input into the euphotic zone, and in turn, the biological response. By further exploring the controls on the physical and biogeochemical life stages of cyclonic eddies, we can better characterize the impacts of a cyclone on nutrient cycling, plankton physiology and variability, and both the silica and carbon budgets of the world's oceans.

Acknowledgments

We thank all E-Flux collaborators, in particular lead PI Claudia Benitez-Nelson and fellow PI's Mike Landry and Carrie Leonard for their significant insights, and Patricia McAndrew and Robert R. Bidigare III for their assistance in collecting the data described in this paper. We also extend our gratitude to the officers and crew of R/V *Ka'imikai-O-Kanaloa* and R/V *Wecoma*. For contributions in analyses we wish to acknowledge Stephanie Christensen, Joe Jennings, Terri Rust, Jamie Tanimoto, Tara Clemente, Holly Rodrigues, and Valerie Franck. We would also like to thank the HOT group, in particular Blake Watkins, Tom Gregory, Eric Grabowski, and Dan Sadler for assistance with the sediment trap. Lastly, we acknowledge the National Science Foundation and the Gordon and Betty Moore Foundation (DMK) for financial support.

References

Anderson, R.A., Bidigare, R.R., Keller, M.D., Latasa, M., 1996. A comparison of HPLC pigment signatures and electron microscopic observations for oligotrophic waters of the North Atlantic and Pacific Oceans. Deep-Sea Research II 43, 517–537.

Armstrong, F.A.J., Stearns, C.R., Strickland, J.D.H., 1967. The measurement of upwelling and subsequent biological processes by means of the Technicon AutoAnalyzer™ and associated equipment. Deep-Sea Research I 14, 381–389.

Atlas, E.L., Hager, S.W., Gordon, L.I., Park, P.K., 1971. A practical manual for use of the Technicon Autoanalyzer ™ in seawater nutrient analyses; revised. Technical Report 215, Oregon State University, Department of Oceanography, Ref. No. 71-22, Unpublished.

Benitez-Nelson, C., Bidigare, R.R., Dickey, T.D., Landry, M.R., Leonard, C.L., Brown, S.L., Nencioli, F., Rii, Y.M., Maiti, K., Becker, J.W., Bibby, T.S., Black, W., Cai, W.J., Carlson, C., Chen, F.Z., Kuwahara, V.S., Mahaffey, C., McAndrew, P.M., Quay, P.D., Rappé, M., Selph, K.E., Simmons, M.E., Yang, E.J., 2007. Eddy-induced diatom bloom drives increased biogenic silica flux, but inefficient carbon export in the subtropical North Pacific Ocean. Science 316, 1017–1021.

Bernhardt, H., Wilhelms, A., 1967. The continuous determination of low level iron, soluble phosphate and total phosphate with the AutoAnalyzer ™. Technicon Symposium, vol. I, Unpublished.

Bidigare, R.R., Trees, C.C., 2000. HPLC phytoplankton pigments: sampling, laboratory methods, and quality assurance procedures. In: Mueller, J.L., Gargion, G. (Eds.), Ocean Optics Protocols for Satellite Ocean Color Sensor Validation, Revision 2, NASA Technical Memo, 2000209966, pp. 154–161.

Bidigare, R.R., Marra, J., Dickey, T.D., Iturriaga, R., Baker, K.S., Smith, R.C., Pak, H., 1990. Evidence for phytoplankton succession and chromatic adaptation in the Sargasso Sea during spring 1985. Marine Ecology Progress Series 60, 113–122.

Bidigare, R.R., Benitez-Nelson, C., Leonard, C.L., Quay, P.D., Parsons, M.L., Foley, D.G., Seki, M.P., 2003. Influence of a cyclonic eddy on microheterotroph biomass and carbon export in the lee of Hawaii. Geophysical Research Letters 30, 51–54.

Bidigare, R.R., Van Heukelem, L., Trees, C.C., 2005. Analysis of algal pigments by high-performance liquid chromatography. In: Andersen, R. (Ed.), Algal Culturing Techniques. Academic Press, New York, pp. 327–345.

Bidigare, R.R., 2008. Subtropical ocean ecosystem structure changes forced by North Pacific climate variation. AGU Joint Assembly Meeting, 27–30 May 2008 (Ft. Lauderdale).

Bienfang, P.K., Ziemann, D.A., Laws, E.A., 1990. Description of a mesoscale eddy in oligotrophic waters off Hawaii. EOS, Transactions, American Geophysical Union 71, 176.

Brown, S.L., Landry, M.R., Neveux, J., Dupouy, C., 2003. Microbial community abundance and biomass along a 180° transect in the equatorial Pacific during an El Niño-Southern Oscillation cold phase. Journal of Geophysical Research 108, 8139–8141.

Brown, S.L., Landry, M.R., Selph, K.E., 2008. Diatoms in the desert: Plankton community response to a subtropical mesoscale eddy in the subtropical North Pacific. Deep-Sea Research II, this issue [doi:10.1016/j.dsr2.2008.02.012].

Brzezinski, M.A., Nelson, D.M., 1995. The annual silica cycle in the Sargasso Sea near Bermuda. Deep-Sea Research I 42, 1215–1237.

Brzezinski, M.A., Nelson, D.M., 1996. Chronic substrate limitation of silicic acid uptake rates in the western Sargasso Sea. Deep-Sea Research II 43, 437–453.

Brzezinski, M.A., Villareal, T.A., Lipschultz, F., 1998. Silica production and the contribution of diatoms to new primary production in the central North Pacific. Marine Ecology Progress Series 167, 89–104.

Brzezinski, M.A., Nelson, D.M., Franck, V.M., Sigmon, D.E., 2001. Silicon dynamics within an intense open-ocean diatom bloom in the Pacific sector of the Southern Ocean. Deep-Sea Research II 48, 3997–4018.

Buesseler, K.O., 1991. Do upper-ocean sediment traps provide an accurate record of particle flux? Nature 353, 420–423.

Buesseler, K.O., Steinberg, D.K., Michaels, A.F., Johnson, R.J., Andrews, J.E., Valdes, J.R., Price, J.F., 2000. A comparison of the quantity and composition of material caught in a neutrally buoyant versus surface-tethered sediment trap. Deep-Sea Research I 47, 277–294.

Butman, C.A., Grant, W.D., Stolzenbach, K.D., 1986. Predictions of sediment trap biases in turbulent flows: a theoretical analysis based on observations from the literature. Journal of Marine Research 44, 601–644.

Calil, P.H.R, Richards, K., Jia, Y., Bidigare, R.R., 2008. Eddy activity in the Lee of the Hawaiian Islands. Deep-Sea Research II, this issue [doi:10.1016/j.dsr2.2008.01.008].

Campbell, L., Vaulot, D., 1993. Photosynthetic picoplankton community structure in the subtropical North Pacific Ocean near Hawaii (station ALOHA). Deep-Sea Research I 40, 2043–2060.

Chavanne, C., Flament, P., Lumpkin, R., Dousset, B., Bentamy, A., 2002. Scatterometer observations of wind variations induced by oceanic islands: implications for wind-driven ocean circulation. Canadian Journal of Remote Sensing 28, 466–474.

Cipollini, P., Cromwell, D., Challenor, P.G., Raffaglio, S., 2001. Rossby waves detected in global ocean colour data. Geophysical Research Letters 28, 466–474.

Clements, F.E., 1916. Plant Succession: an Analysis of the development of Vegetation. Carnegie Institute of Washington.

DeMaster, D.J., 1981. The supply and accumulation of silica in the marine environment. Geochimica et Cosmochimica Acta 45, 1715–1732.

Dickey, T., Nencioli, F., Kuwahara, V., Leonard, C., Black, W., Bidigare, R., Rii, Y., Zhang, Q., 2008. Physical and bio-optical observations of oceanic cyclones west of the island of Hawai'i. Deep-Sea Research II, this issue [doi:10.1016/j.dsr2.2008.01.006].

Egge, J.K., Aksnes, D.L., 1992. Silicate as regulating nutrient in phytoplankton competition. Marine Ecology Progress Series 83, 281–289.

Eppley, R.W., 1969. Comparison of half-saturation constants for growth and nitrate uptake of marine phytoplankton. Journal of Phycology 5, 375.

Eppley, R.W., Peterson, B.J., 1979. Particulate organic matter flux and planktonic new production in the deep ocean. Nature 282, 677–680.

Falkowski, P.G., Ziemann, D.A., Kolber, Z., Bienfang, P.K., 1991. Role of eddy pumping in enhancing primary production in the ocean. Nature 352, 55–58.

Flierl, G., McGillicuddy, D.J., 2002. Mesoscale and submesoscale physical–biological interactions. In: Robinson, A.R., McCarthy, J.J., Rothschild, B.J. (Eds.), The Sea. Wiley, New York, pp. 113–186.

Garçon, V.C., Oschlies, A., Doney, S.C., McGillicuddy, D.J., Waniek, J., 2001. The role of mesoscale variability on plankton dynamics in the North Atlantic. Deep-Sea Research I 48, 2199–2226.

Goldman, J.C., 1988. Spatial and temporal discontinuities of biological processes in pelagic surface waters. In: Rothschild, B.J. (Ed.), Towards a Theory on Biological–Physical Interactions in the World Ocean. Springer, New York, pp. 273–296.

Goldman, J.C., 1993. Potential role of large oceanic diatoms in new primary production. Deep-Sea Research I 40, 159–168.

Gordon, L.I., Jennings, J.C., Ross, A.A., Krest, J.M., 1994. A suggested protocol for continuous flow analysis of seawater nutrients (phosphate, nitrate, nitrite, and silicic acid) in the WOCE Hydrographic Program and Joint Global Ocean Fluxes Study. WHP Office Report 91-1, Unpublished.

Guillard, R.R.L., 1975. Culture of phytoplankton for feeding marine invertebrates. In: Smith, W.L., Chaney, M.H. (Eds.), Culture of Marine Invertebrate Animals. Plenum Press, New York, pp. 29–60.

Henson, S.A., Sanders, R., Holeton, C., Allen, J.T., 2006. Timing of nutrient depletion, diatom dominance and a lower-boundary estimate of export production for Irminger Basin, North Atlantic. Marine Ecology Progress Series 313, 73–84.

Honjo, S., Dymond, J., Prell, W., Ittekot, V., 1999. Monsoon-controlled export fluxes to the interior of the Arabian Sea. Deep-Sea Research II 46, 1859–1902.

Hutchinson, G.E., 1961. The paradox of the plankton. American Naturalist 95, 137.

Jeffrey, S.W., Vesk, M., 1997. Introduction to marine phytoplankton and their pigment signatures. In: Jeffrey, S.W., Mantoura, R.F.C., Wrights, S.W. (Eds.), Phytoplankton Pigments in Oceanography: Guidelines to Modern Methods. UNESCO, Paris, pp. 37–84.

Karl, D.M., 2002. Nutrient dynamics in the deep blue sea. Trends in Microbiology 10, 410–418.

Karl, D.M., Christian, J.R., Dore, J.E., Hebel, D.V., Letelier, R.M., Tupas, L.M., Winn, C.D., 1996. Seasonal and interannual variability in primary production and particle flux at Station ALOHA. Deep-Sea Research II 43, 539–568.

Karl, D.M., Bidigare, R.R., Letelier, R.M., 2001a. Long-term changes in plankton community structure and productivity in the North Pacific Subtropical Gyre: the domain shift hypothesis. Deep-Sea Research II 48, 1449–1470.

Karl, D.M., Bjorkman, K.M., Dore, J.E., Fujieki, L., Hebel, D.V., Houlihan, T., Letelier, R.M., Tupas, L.M., 2001b. Ecological nitrogen-to-phosphorus stoichiometry at Station ALOHA. Deep-Sea Research II 48, 1529–1566.

Karl, D.M., Bidigare, R.R., Letelier, R.M., 2002. Sustained and aperiodic variability in organic matter production and phototrophic microbial community structure in the North Pacific Subtropical Gyre. In: le B. Williams, P.J., Thomas, D.N., Reynolds, C.S. (Eds.), Phytoplankton Productivity, Carbon Assimilation in Marine and Freshwater Ecosystems. Blackwell Science Ltd., Malden, pp. 222–264.

Knauer, G.A., Martin, J.H., Bruland, K., 1979. Fluxes of particulate carbon, nitrogen, and phosphorus in the upper water column of the Northeast Pacific Ocean. Deep-Sea Research 26, 97–108.

Kuwahara, V.S., Nencioli, F., Dickey, T.D., Rii, Y.M., Bidigare, R.R., 2008. Physical dynamics and biological implications of cyclonic eddy *Noah* in the lee of Hawaii during E-Flux I. Deep-Sea Research II, this issue [doi:10.1016/j.dsr2.2008.01.007].

Landry, M.R., Brown, S.L., Rii, Y.M., Selph, K.E., Bidigare, R.R., Yang, E.J., Simmons, M.P., 2008. Depth-stratified phytoplankton dynamics in Cyclone *Opal*, a subtropical mesoscale eddy. Deep-Sea Research II, this issue [doi:10.1016/j.dsr2.2008.02.001].

Laws, E.A., Falkowski, P.G., Smith, R.C., Ducklow, H., McCarthy, J.J., 2000. Temperature effects on export production in the open ocean. Global Biogeochemical Cycles 14, 1231–1246.

Legendre, L., Le Fevre, J., 1995. Microbial food webs and the export of biogenic carbon in oceans. Aquatic Microbial Ecology 9, 69–77.

Letelier, R.M., Bidigare, R.R., Hebel, D.V., Ondrusek, M.E., Winn, C.D., Karl, D.M., 1993. Temporal variability of phytoplankton community structure based on pigment analysis. Limnology and Oceanography 38, 1420–1437.

Lewis, M.R., 2002. Variability of plankton and plankton processes on the mesoscale. In: le B. Williams, P.J., Thomas, D.N., Reynolds, C.S. (Eds.), Phytoplankton Productivity, Carbon Assimilation in Marine and Freshwater Ecosystems. Blackwell Science Ltd., Malden, pp. 141–155.

Lumpkin, C.F., 1998. Eddies and currents of the Hawaiian Islands. Ph.D. Dissertation, School of Ocean and Earth, Science and Technology, University of Hawai'i at Manoa, Honolulu, Unpublished.

Mahaffey, C., Benitez-Nelson, C.R., Bidigare, R., Rii, Y., Karl, D.M., 2008. Nitrogen dynamics within a wind-driven eddy. Deep-Sea Research II, this issue [doi:10.1016/j.dsr2.2008.02.004].

Maiti, K., Benitez-Nelson, C., Rii, Y.M., Bidigare, R.R., 2008. Influence of a mature cyclonic eddy on particle export in the lee of Hawai'i. Deep-Sea Research II, this issue [doi:10.1016/j.dsr2.2008.02.008].

Mantoura, R.F.C., Llewellyn, C.A., 1983. The rapid determination of algal chlorophyll and carotenoid pigments and their breakdown products in natural waters by reverse-phase high-performance liquid chromatography. Analytica Chimica Acta 151, 297–314.

McCave, I.N., 1975. Vertical flux of particles in the ocean. Deep-Sea Research 22, 491–502.

McGillicuddy, D.J., Robinson, A.R., 1997. Eddy-induced nutrient supply and new production in the Sargasso Sea. Deep-Sea Research I 44, 1427–1450.

McGillicuddy, D.J., Anderson, L.A., Bates, N.R., Bibby, T., Buesseler, K.O., Carlson, C.A., Davis, C.S., Ewart, C., Falkowski, P.G., Goldthwait, S.A., Hansell, D.A., Jenkins, W.J., Johnson, R., Kosnyrev, V.K., Ledwell, J.R., Li, Q.P., Siegel, D.A., Steinberg, D.K., 2007. Eddy/wind interactions stimulate extraordinary mid-ocean plankton blooms. Science 316, 1021–1026.

McNeil, J.D., Jannasch, H.W., Dickey, T.D., McGillicuddy, D., Brzezinski, M., Sakamoto, C.M., 1999. New chemical, bio-optical and physical observations of upper ocean response to the passage of a mesoscale eddy off Bermuda. Journal of Geophysical Research 104, 15537–15548.

Morel, A., 1988. Optical modeling of the upper ocean in relation to its biogenous matter content (Case I waters). Journal of Geophysical Research 93, 10749–10768.

Nencioli, F., Dickey, T.D., Kuwahara, V.S., Black, W., Rii, Y.M., Bidigare, R.R., 2008. Physical dynamics and biological implications of a mesoscale cyclonic eddy in the lee of Hawaii: Cyclone *Opal* observations during E-Flux III. Deep-Sea Research II, this issue [doi:10.1016/j.dsr2.2008.02.003].

Noble, A.E., Saito, M.A., Maiti, K., Benitez-Nelson, C.R., 2008. Cobalt, manganese, and iron near the Hawaiian Islands: a potential concentrating mechanism for cobalt within a cyclonic eddy and implications for the hybrid-type trace metals. Deep-Sea Research II, this issue [doi:10.1016/j.dsr2.2008.02.010].

Olaizola, M., Ziemann, D.A., Bienfang, P.K., Walsh, W.A., Conquest, L.D., 1993. Eddy-induced oscillations of the pycnocline affect the floristic composition and depth distribution of phytoplankton in the subtropical Pacific. Marine Biology 116, 533–542.

Ondrusek, M.E., Bidigare, R.R., Sweet, S.T., Defreitas, D.A., Brooks, J.M., 1991. Distribution of phytoplankton pigments in the North Pacific Ocean in relation to physical and optical variability. Deep-Sea Research 38, 243–266.

Paasche, E., 1980. Silicon content of five marine plankton diatom species measured with a rapid filter method. Limnology and Oceanography 25, 474–480.

Patzert, W.C., 1969. Eddies in Hawaiian waters. HIG Technical Report 69-8, Hawai'i Institute of Geophysics, University of Hawai'i, Honolulu, Hawai'i, Unpublished.

Petersen, R., 1975. Paradox of plankton—equilibrium hypothesis. American Naturalist 109, 35.

Sakamoto, C.M., Karl, D.M., Jannasch, H.W., Bidigare, R.R., Letelier, R.M., Walz, P.M., Ryan, J.P., Polito, P.S., Johnson, K.S., 2004. Influence of Rossby waves on nutrient dynamics and the plankton community structure in the North Pacific subtropical gyre. Journal of Geophysical Research 109.

Scharek, R., Latasa, M., Karl, D.M., Bidigare, R.R., 1999a. Temporal variations in diatom abundance and downward vertical flux in the oligotrophic North Pacific gyre. Deep-Sea Research I 46, 1051–1075.

Scharek, R., Tupas, L.M., Karl, D.M., 1999b. Diatom fluxes to the deep sea in the oligotrophic North Pacific gyre at Station ALOHA. Marine Ecology Progress Series 182, 55–67.

Seki, M.P., Polovina, J.J., Brainard, R.E., Bidigare, R.R., Leonard, C.L., Foley, D.G., 2001. Biological enhancement at cyclonic eddies tracked with GOES thermal imagery in Hawaiian waters. Geophysical Research Letters 28, 1583–1586.

Sharp, J.H., 1974. Improved analysis for particulate organic carbon and nitrogen from seawater. Limnology and Oceanography 19, 984–989.

Siegel, D.A., 2001. The Rossby rototiller. Nature 409, 576–577.

Strickland, J.D.H., Parsons, T.R., 1972. A practical handbook of seawater analysis. Fisheries Research Board of Canada, Unpublished.

Sweeney, E.N., McGillicuddy, D.J., Buesseler, K.O., 2003. Biogeochemical impacts due to mesoscale eddy activity in the Sargasso Sea as measured at the Bermuda Atlantic Time-series Study (BATS). Deep-Sea Research II 50, 3017–3039.

Tilman, D., 1980. Resources: a graphical-mechanistic approach to competition and predation. American Naturalist 116, 362–393.

Turpin, D.H., Harrison, P.J., 1979. Limiting nutrient patchiness and its role in phytoplankton ecology. Journal of Experimental Marine Biology and Ecology 39, 151–166.

Uz, B.M., Yoder, J.A., Osychny, V., 2001. Pumping of nutrients to ocean surface waters by the action of propagating planetary waves. Nature 409, 597–600.

Vaillancourt, R.D., Marra, J., Seki, M.P., Parsons, M.L., Bidigare, R.R., 2003. Impact of a cyclonic eddy on phytoplankton community structure and photosynthetic competency in the subtropical North Pacific Ocean. Deep-Sea Research I 50, 829–847.

Verdeny, E., Masqué, P., Maiti, K., Garcia-Orellana, J., Bruach, J.M., Mahaffey, C., Benitez-Nelson, C.R., 2008. Particle export within cyclonic Hawaiian lee eddies derived from ^{210}Pb–^{210}Po disequilibria. Deep-Sea Research II, this issue [doi:10.1016/j.dsr2.2008.02.009].

Wright, S.W., Jeffrey, S.W., Mantoura, R.F.C., Llewellyn, C.A., Bjornland, T., Repeta, D., Welschmeyer, N., 1991. Improved HPLC method for the analysis of chlorophylls and carotenoids from marine phytoplankton. Marine Ecology Progress Series 77, 183–196.